To the Graduate Council:

I am submitting herewith a dissertation written by Robert Sherwood Howell entitled "Equivalent Source Estimation for use in Solving the Fixed Source Boltzmann Transport Euqation by Monte Carlo Methods." I recommend that it be accepted in partial fulfillment of the requirements for the degree of Doctor of Philosophy, with a major in Nuclear Engineering.

Paul N. Stevens, Major Professor

We have read this dissertation and recommend its acceptance:

Victor R. Cain

P. F. Gasqua

Laurence F. Miller

T. A. Welton

Accepted for the Council:

Vice Chancellor
Graduate Studies and Research

4

EQUIVALENT SOURCE ESTIMATION FOR USE IN SOLVING THE FIXED SOURCE BOLTZMANN TRANSPORT EQUATION BY MONTE CARLO METHODS

A Dissertation

Presented for the

Doctor of Philosophy

Degree

The University of Tennessee, Knoxville

Robert Sherwood Howell

June 1981

3051898

ACKNOWLEDGEMENTS

The author sincerely thanks Dr. P. N. Stevens, who served as his major professor, for his invaluable guidance and encouragement throughout this work. The assistance and encouragement which he received from all the members of his committee is genuinely appreciated.

This work was supported by the Oak Ridge office of Science Applications, Incorporated. The author gratefully acknowledges the numerous SAI staff members who assisted in providing the funding for this research. Further, the excellent work of Patricia Hamrick, in typing this document, is sincerely appreciated.

The course of study and research leading to this document could not have been completed without the patience, understanding, and encouragement of the author's family. For this reason and for the happiness they have provided, this dissertation is dedicated to his wife, Donna, and sons, Aaron and Corey.

ABSTRACT

Two surface equivalent source estimators were developed for Monte Carlo solution of the fixed source Boltzmann transport equation. These estimators are analogous to the contributon Monte Carlo estimator, i.e., volume equivalent source estimator. The surface estimation schemes were calculationally demonstrated to provide superior precision and benefit over contributon Monte Carlo for full transport calculations. They were also demonstrated to be applicable to void streaming calculations in which transport in the surrounding medium was replaced with albedo surfaces. Using a surface equivalent source estimator, the variance reduction mechanisms of contributon Monte Carlo and surface equivalent source estimation were investigated and shown to be equivalent to those of the standard biasing scheme, splitting.

The combination of simultaneously calculated standard and equivalent source estimates of the response was formally investigated. It was shown that the conditions for optimized combination of these estimates are restricted such that combinations in most cases would not result in a significant gain in benefit.

Guidelines, primarily for use of the vacuum surface equivalent source estimator, were formulated based on the understanding of the variance reduction mechanisms developed in this research, calculational experience obtained in this work, and previously reported experience with contributon Monte Carlo and surface splitting. The guidelines are not, in general, expected to provide optimum results but will provide the insight and guidance to allow significant gains in benefit from use of the procedure in either full transport or void streaming problems.

TABLE OF CONTENTS

CHAPTER		PAGE
I.	INTRODUCTION	1
II.	GENERAL TRANSPORT AND CONTRIBUTON BACKGROUND INFORMATION	4
	The Adjoint Function	4
	Calculation of Response Using the Value Functions	5
	Chronological Review of Recent Developments Leading to Contributon Monte Carlo	8
	Overview of Developments in Contributon Monte Carlo	11
III.	FORMAL BASIS FOR TRACKING AND ESTIMATION PROCEDURES	18
IV.	COMPARISON OF BENEFIT PRODUCING MECHANISMS IN ESP ESTIMATION AND SPLITTING	23
	Surface ESP Estimation	23
	Method of Benefit Production	26
V.	PARAMETRIC STUDIES AND COMPARISONS BETWEEN VOLUME AND SURFACE EQUIVALENT SOURCE ESTIMATION FOR FULL TRANSPORT CALCULATIONS	29
	Code Benchmarks	30
	Parametric Studies for Analog Calculations	31
	Parametric Studies for Biased Calculations	43
	Discussion of Results	49
	Summary	55
VI.	APPLICATION OF VACUUM SURFACE EQUIVALENT SOURCE ESTIMATION TO VOID STREAMING CALCULATIONS	57
	Problem Description	57
	Results and Discussion	62
VII.	INVESTIGATION OF THE FEASIBILITY OF COMBINING SIMULTANEOUSLY CALCULATED STANDARD AND EQUIVALENT SOURCE RESPONSE ESTIMATES	69
	Concepts of Combining Correlated Estimates	69
	Application of Concepts and Discussion	78
VIII.	GENERAL GUIDELINES FOR USE OF EQUIVALENT SOURCE ESTIMATION	85
	Fundamental Principles of Equivalent Source Estimation	86
	General Guidance of a Problem Specific Nature	88
	Summary	98
IX.	CONCLUSIONS AND RECOMMENDATIONS FOR FUTURE WORK	101
LIST OF REFERENCES		105
VITA		108

LIST OF TABLES

TABLE		PAGE
V-1.	Summary of Results for Variations in Position of a 2 mfp Thick Volume of Integration	34
V-2.	Summary of Results for Variations in the Normal Thickness of the Volume of Integration	38
V-3.	Summary of Results for the Biased Full Transport Calculations	47
VI-1.	Summary of Results for Two-Legged Duct Geometry	63
VII-1.	Combination of Results for the Parametric Study on Volume of Integration Position	79
VII-2.	Combination of Results for the Parametric Study on Volume of Integration Thickness	80
VII-3.	Combination of Results for the Parametric Studies with Biased Calculations	82
VII-4.	Combination of Results for Two-Legged Duct Void Streaming Calculations	83

LIST OF FIGURES

FIGURE		PAGE
V-1.	Variance as a function of ESP volume distance from center of sphere - 2 mfp volume thickness	35
V-2.	$\sigma^2 T$ as a function of ESP volume distance from center of sphere - 2 mfp volume thickness	36
V-3.	Variance as a function of ESP volume thickness - volume center 7.5 mfp from sphere center	39
V-4.	$\sigma^2 T$ as a function of volume thickness - volume center 7.5 mfp from sphere center	40
V-5.	Variance and $\sigma^2 T$ as functions of volume thickness - biased calculations; volume centered at 12 mfp	48
VI-1.	Combinatorial geometry model of two-legged duct	58
VI-2.	Variance and time as functions of ESP/SP ratio - ESP surface located at 13.5 feet	64
VI-3.	$\sigma^2 T$ as a function of ESP/SP ratio - equivalent source located at 13.5 feet	65
VII-1.	Ratio of variance-comb/variance-ESP as a function of the ratio variance-std/variance-ESP and correlation	73
VII-2.	Correlation coefficient as a function of the ratio variance-std/variance-ESP for variance-comb/ variance-ESP = 1.0	74

CHAPTER I

INTRODUCTION

One of the primary concerns with the use of Monte Carlo simulation is the precision of the estimate. This concern is enhanced in Monte Carlo solutions of the fixed source Boltzmann transport equation for deep penetration type problems because of the large attenuations and hence excessive computing times required to obtain sufficient statistical accuracy. As a result, much effort has been expended on developing variance reduction techniques for this class of problem. One such technique, contributon Monte Carlo estimation, which is based on a volume integral over an adjoint weighted volume equivalent source, was developed at Los Alamos Scientific Laboratory by Dubi and Gerstl.[1] Since its development, considerable controversy has mounted concerning the effectiveness and use of the method. It is clear, however, that much of the concern has developed as a result of a lack of knowledge of the actual variance reduction mechanism. The work reported in the following chapters consists of a clarification and extension of that performed by Dubi and Gerstl.

This research has been directed toward four fundamental objectives:

1. Formal development of an understanding of the variance reduction mechanism in equivalent source estimation, i.e., contributon Monte Carlo.
2. Development and comparison of an analogous procedure based on surface-crossing generated equivalent source particles.

3. Investigation of the feasibility of combining the simultaneously calculated standard and equivalent source estimates of the response to gain a more precise estimate.
4. Development of general guidelines for use of the equivalent source estimators.

Completion of the first three objectives, in combination with previous investigations, provides a sufficient understanding of the technique for the development of general guidelines (objective four) which are necessary for efficient use of the estimators. In addition, accomplishment of the second objective provides a more precise estimator which is also suitable for use with albedo surfaces in void streaming calculations.

Chapter II provides a review of some of the concepts, notations, and terminology that are fundamental to this work and further presents a review of previous developments and investigations. Chapter III provides insight into contributon Monte Carlo through the formal bases of the tracking procedure, while Chapter IV formally investigates the variance reduction mechanism and develops the analogous surface equivalent source procedure. Results of calculations aimed at comparing the surface and volume equivalent source procedures along with providing needed information for development of guidelines for efficient use of the procedures in both full transport and void streaming problems are presented in Chapters V and VI. The feasibility of combining simultaneously calculated responses produced by the standard and equivalent source estimators is investigated in Chapter VII. Information gained from work performed in Chapters IV through VII is combined in

Chapter VIII, along with experience gained by other investigators, to develop general guidelines for efficient use of the technique. The final chapter, Chapter IX, presents the conclusions and provides recommendations for future work in the area of equivalent source estimation.

CHAPTER II

GENERAL TRANSPORT AND CONTRIBUTON BACKGROUND INFORMATION

The purpose of this chapter is two-fold. The first is a review of some of the concepts, notations, and terminology of transport theory. The second is a chronological review of the development of contributon theory and contributon Monte Carlo estimation.

1. The Adjoint Function

The following time-independent form of the adjoint Boltzmann transport equation and the appropriate boundary conditions defines the adjoint function, $\phi^*(\bar{r},E,\bar{\Omega})$,

$$-\bar{\Omega}\cdot\bar{\nabla}\phi^*(\bar{r},E,\bar{\Omega}) + \Sigma_t(\bar{r},E)\phi^*(\bar{r},E,\bar{\Omega}) = S^*(\bar{r},E,\bar{\Omega}) + \int\int dE'd\bar{\Omega}'\Sigma_s(\bar{r},E\rightarrow E',\bar{\Omega}\rightarrow\bar{\Omega}')\phi^*(\bar{r},E',\bar{\Omega}'), \qquad \text{(II-1)}$$

where:

$\phi^*(\bar{r},E,\bar{\Omega})$ is the adjoint function,

$\Sigma_t(\bar{r},E)$ is the total cross section,

$\Sigma_s(\bar{r},E\rightarrow E',\bar{\Omega}\rightarrow\bar{\Omega}')$ is the scattering cross section, and

$S^*(\bar{r},E,\bar{\Omega})$ is the adjoint source.

This form of the adjoint equation is derived in such references as Henry,[2] Bell and Glasstone,[3] and Straker, et al.[4] It has been shown by Straker, et al.[4] that the function given by equation II-1 is not adjoint to the flux, $\phi(\bar{r},E,\bar{\Omega})$ but rather to the emergent particle density, $\chi(\bar{r},E,\bar{\Omega})$. When the response function per unit flux is used as the

adjoint source, $\phi^*(\bar{r},E,\bar{\Omega})$ is the value of future contributions to the effect of interest from a source particle emerging at point $\bar{r}$, with direction $\bar{\Omega}$, and energy E and is referred to as the point value.[4,5] An analogous function, the event value, $W(\bar{r},E,\bar{\Omega})$, has been derived and gives the value of present and future contributions to the effect of interest of a particle entering a first collision at point $\bar{r}$, with energy E, and direction $\bar{\Omega}$.[4,5,6] As implied by the definitions of $\phi^*(\bar{r},E,\bar{\Omega})$ and $W(\bar{r},E,\bar{\Omega})$ there exists a relatively simple relationship between the two value functions. This relationship, as presented in reference 5, is shown by the following,

$$\phi^*(\bar{r},E,\bar{\Omega}) = \int \Sigma_t(\bar{r}',E) \exp\left[-\int_0^R \Sigma_t(\bar{r}+R'\bar{\Omega})dR'\right] \times W(\bar{r}',E,\bar{\Omega})dR, \qquad \text{(II-2)}$$

where:

$\bar{r}'$ is the first collision point following emission at $\bar{r}$,

R is the distance between $\bar{r}$ and $\bar{r}'$, i.e., $\bar{r}' = \bar{r} + R\bar{\Omega}$, and

all other terms are the same as previously defined.

The physical differences in these value functions is significant and is relied upon heavily in the development in Chapter III.

2. Calculation of Response Using the Value Functions

In transport calculations the effect of interest, I, may be calculated in various ways depending on the physical problem. The usual method is through the integration of the product of the forward flux and a response function. This functional is given by the equation,

$$I = \left\langle \phi(\bar{r},E,\bar{\Omega}),R(\bar{r},E) \right\rangle , \qquad \text{(II-3)}$$

where:

< > indicates integration over all phase space,

$\phi(\bar{r},E,\bar{\Omega})$ is the forward flux, and

$R(\bar{r},E)$ is the response function per unit flux.

Several mathematically equivalent methods of calculating the response by using the value functions are well known and are discussed in the remainder of this section.

The most common method for calculating the effect of interest using the value functions is the integration of the product of the point value and a source function. This functional is presented in equation II-4 and is derived and discussed in references 2, 3, 7, and 8,

$$I = \left\langle S(\bar{r},E,\bar{\Omega}),\phi^*(\bar{r},E,\bar{\Omega}) \right\rangle , \qquad \text{(II-4)}$$

where:

$S(\bar{r},E,\bar{\Omega})$ is the fixed source for the forward transport equation,

and

$\phi^*(\bar{r},E,\bar{\Omega})$ is the point value as calculated by equation II-1.

The relationship in equation II-4 is seen to be fully consistent with the definition of the point value. A less familiar relationship analogous to equation II-4 which involves the event value is given by the following equation,[6]

$$I = \left\langle S_c(\bar{r},E,\bar{\Omega}),W(\bar{r},E,\bar{\Omega}) \right\rangle , \qquad \text{(II-5)}$$

where:

$S_c(\bar{r},E,\bar{\Omega})$ is the first-collision source, and

$W(\bar{r},E,\bar{\Omega})$ is the event value.

A third method for calculating the effect of interest is through the surface interal given in the equation,[8,9]

$$I = \iiint_S \bar{n}\cdot\bar{\Omega}\phi(\bar{r},E,\bar{\Omega})\phi^*(\bar{r},E,\bar{\Omega})dS d\bar{\Omega} dE, \qquad \text{(II-6)}$$

where:

S represents a closed surface where the enclosed volume contains either the source or the detector, but not both,

$\bar{n}$ is the unit normal vector of the surface S (outward normal if S encloses the source and inward normal if S encloses the detector),

$\bar{\Omega}$ is the particle direction vector,

$\phi(\bar{r},E,\bar{\Omega})$ is the forward flux, and

$\phi^*(\bar{r},E,\bar{\Omega})$ is the adjoint flux (point value).

The application of this method has been discussed by Hoffman[10] and Williams and Engle.[7] It is important to note that the $\bar{n}\cdot\bar{\Omega}\phi(\bar{r},E,\bar{\Omega})$ term in equation II-6 forms an equivalent source at the surface S, thus producing emergent source particles.[9] The weighting of $\bar{n}\cdot\bar{\Omega}\phi(\bar{r},E,\bar{\Omega})$ by the point value to produce the effect of interest is therefore consistent with the definition discussed in Section 1. The relationship between the surface integral method and the contributon Monte Carlo method, discussed in the next section, will be used extensively in later chapters.

3. Chronological Review of Recent Developments Leading to Contributon Monte Carlo

The use of the term contributon was initiated by Williams and Engle in their development of spatial channel theory.[7] Williams and Engle used the "global reciprocity theorem," as follows,

$$\left\langle \phi^*(\bar{p}),Q(\bar{p}) - \phi(\bar{p}),Q^*(\bar{p}) \right\rangle = \oint_A dA \int_E \int_\Omega \bar{n}\cdot\bar{\Omega}\phi\phi^*(\bar{p})d\bar{\Omega}dE, \qquad \text{(II-7)}$$

to demonstrate that the response was given by equation II-8, i.e., the previously discussed surface integral method,

$$\int_{\substack{A \\ Z=Z_o}} \left\{ \int_E \int_\Omega (\bar{n}\cdot\bar{\Omega})\phi(\bar{\Omega},E,Z,X)\phi^*(\bar{\Omega},E,Z,X)d\bar{\Omega}dE \right\} dA = \left\langle \phi,Q^* \right\rangle , \qquad \text{(II-8)}$$

where:

$Q(\bar{p})$ is the source for the forward equation,

$Q^*(\bar{p})$ is the source for the adjoint equation,

A is an arbitrarily located plane, $Z = Z_o$, between the source and detector, and

all other terms are the same as previously defined.

From equation II-8, $\int_E \int_\Omega \bar{\Omega}\phi(\bar{p})\phi^*(\bar{p})d\bar{\Omega}dE$ was defined as $\bar{D}(X,Z)$ and was considered to be the current of special particles which Williams and Engle defined as "contributons." Then C(x,z), given by equation II-9, is the "contributon flux," i.e., the flux of particles that will certainly contribute to the response,

$$C(x,z) = \int_E \int_\Omega \phi(\bar{p})\phi^*(\bar{p})d\bar{\Omega}dE \ . \qquad \text{(II-9)}$$

It should be noted that $\bar{n}\cdot\bar{D}(x,z)$ produces the response per unit area. Williams and Engle observed that plots of $\bar{n}\cdot\bar{D}(x,z)$, along arbitrary z planes between the source and detector, or the spatial distribution of $C(x,z)$ will identify spatial streaming paths. The usefulness of these plots has been demonstrated considering both simple and very complex geometries.

Williams and Engle's work was closely followed with a related development by S.A.W. Gerstl.[8] In this work a conservation law for "ψ-particles" (equivalent to contributons) was postulated. As a result of the conservation law, the distribution of "ψ-particles" was interpreted as describing the field of particles all of which contribute to the detector response. The possible advantages of directly calculating the "ψ-particle" distribution and associated detector response led Gerstl to develop two "ψ-particle transport equations." The first of these equations, equation II-10, is a linear equation which defines the complex variable Ψ and is restricted to slab geometry, monoenergetic transport, and isotropic scattering,

$$-\mu^2 \frac{\partial^2\Psi(x,\mu)}{\partial x^2} + \Sigma^2 \Psi(x,\mu) = (\Sigma - c\mu)S$$

$$+ \frac{c}{2}\mu \int_{-1}^{+1} \left[\frac{\Sigma}{\mu'} \Psi(x,\mu') - \frac{c}{2\mu'} \int_{-1}^{+1} \Psi(x,\mu'') \, d\mu'' \right] d\mu', \qquad \text{(II-10)}$$

where:

$$\Psi(x,\mu) = \phi(x,\mu) + i\phi^*(x,\mu),$$

$S = Q + iR$

$i = \sqrt{-1}$

Q = forward source

R = adjoint source, and

$\phi\phi^*$, i.e., ψ, is given by 1/2 Im Ψ^2.

Gerstl's second equation, equation II-11, defines the real variable ψ but is nonlinear and again is restricted to slab geometry and monoenergetic transport as well as having the further restriction of a purely absorbing medium,

$$\mu^4 \left(\frac{\partial^2\psi}{\partial x^2}\right)^2 + 4\mu^2 QR \frac{\partial^2\psi}{\partial x^2} - \mu^2\Sigma^2\left(\frac{\partial\psi}{\partial x}\right)^2 - 4\Sigma^2 QR\psi + 4Q^2R^2 = 0, \qquad \text{(II-11)}$$

where:

Ψ is the $\phi\phi^*$ product,

Q is the forward source, and

R is the adjoint source.

The complexities of these "transport equations" and their lack of generality leaves little hope for direct solution of the "ψ-particle" distribution and thus the direct solution of the response by the surface integral of $\bar{n}\cdot\bar{\Omega}\psi$ for other than the most trivial cases.

More recently, Deutsch and Carter used spatial channel theory as a basis to develop a Monte Carlo procedure to simultaneously calculate the ϕ and ϕ^* distributions.[11] This procedure results in estimates of $C(x,z)$ for discrete segments of surfaces between the source and detector. Thus, producing spatial channel plots for three dimensional geometries and

forming the procedural basis for directly calculating the $\phi\phi^*$ or "ψ-particle" distribution.

4. Overview of Developments in Contributon Monte Carlo

Dubi, et al.,[1] developed a Monte Carlo scheme for estimating the volume integral of the contributon flux based on a single forward calculation. The unbiased estimator developed by Dubi is given by the equation,

$$\eta(p_1,\ldots,p_n) = \sum_{i=1}^{n} \frac{\chi(\bar{r}_i)}{\Sigma_t(\bar{r}_i)} \xi_F^*(p_i,p_1^i,\ldots,p_k^i), \qquad \text{(II-12)}$$

where:

$p_1,p_2,\ldots,p_n$ denotes the primary particle's history,

$p_i,p_1^i,p_2^i,\ldots,p_k^i$ denotes the history of the secondary particle generated at p_i, i.e., the phase space coordinates of the i^{th} interaction of the primary particle,

$$\chi(\bar{r}_i) = \begin{cases} 1 \text{ for } r \in V \\ 0 \text{ for } r \notin V, \end{cases}$$

V is a volume completely separating the source and detector, but containing neither the source nor detector,

$\Sigma_t(\bar{r}_i)$ is the total scattering cross section,

$$\xi_F^*(p_i,p_1^i,p_2^i,\ldots,p_k^i) = \sum_{j=1}^{K} g(p_j^i),$$

$$g(p_j^i) = \frac{R(p_j^i)}{\Sigma_t(p_j^i)}, \text{ and}$$

$R(p_j^i)$ is the response function per unit flux for the j^{th} interaction of the secondary particle generated at p_i.

The Monte Carlo realization of the quantity $\xi_F^*(p_i,p_1^i,p_2^i,\ldots,p_k^i)$ is accomplished by generating a secondary particle at every collision site of the primary particle within the volume V and tracking the secondary particles in the forward mode. Based on the surface integral of $\bar{n}\cdot\bar{\Omega}\phi\phi^*$, Dubi made the natural extension of the estimator $\eta(p_1,p_2,\ldots,p_n)$ to an estimator of the response as a volume integral as shown for spherical geometry by the equation,

$$\langle \eta_F \rangle = I(R_2-R_1) = \int_{R_1}^{R_2} d\bar{r} \left\{ \int_{4\pi} d\bar{\Omega} \oint_S dS\ \bar{n}\cdot\bar{\Omega}\phi(\bar{r},\bar{\Omega})\phi^*(\bar{r},\bar{\Omega}) \right\} , \qquad \text{(II-13)}$$

where:

I is the response,

R_1 and R_2 are the radii of the inner and outer surfaces, respectively, defining the volume of integration, and

all other terms are the same as previously defined.

It is important to note that equation II-13 may be generalized such that the volume of integration is not required to be a spherical shell. However, the volume of integration is restricted to those geometries which have a uniform spacing between the inner and outer surfaces.

In an effort to determine the usefulness of the scheme, Dubi developed a benefit factor based upon the ratio of σ^2T for regular Monte Carlo to σ^2T for contributon Monte Carlo. Dubi's analytic benefit factor for analog calculations is given by the following equation,

$$B = \frac{N_{eff}}{N_{s,out}\left(1 + \frac{2N_{s-}}{N_{eff}}\right)} \frac{\beta_c}{\beta_p} , \qquad \text{(II-14)}$$

where:

$N_{eff} = N_{s,out} - 2N_{s-}$,

$N_{s,out}$ is the number of secondaries escaping the medium,

N_{s-} is the number of secondaries giving negative contributions,

β_p is the escape probability of primary particles ($N_{p,out}/N_p$), and

β_c is the escape probability of contributing particles.

The response used to develop this benefit factor was the leakage from a homogeneous sphere with a point isotropic source at the center and a vacuum boundary at the surface of the sphere.

The effectiveness of Dubi's procedure was demonstrated by comparison with standard analog Monte Carlo calculations. The demonstration problem geometries consisted of slabs which varied in thickness from 10 to 25 mean free paths (mfp) and spheres with radii which varied from 10 to 35 mfp. The benefit factors, from the Monte Carlo calculations, were shown to range from 5.3 to 8.08 for the slabs and 1.14 to 10.1 for the spheres.

In a later effort, Dubi and Gerstl[12] concentrated on the development of an analytic benefit factor for use when biasing is applied to both the regular and contributon Monte Carlo schemes. Both a semi-intuitive model and a formal development were presented. The benefit factor was again based upon the ratio of the $\sigma^2 T$ indicators of effectiveness. The formal development results in the relatively simple factor given by the equation,

$$B = \Sigma_t^* \Delta \, (1 + \beta N_s/N_p)^{-1} \, , \qquad \text{(II-15)}$$

where:

Σ_t^* is the biased energy independent total cross section; in particular $\Sigma_t^* = \Sigma_t(1-P)$, $0 \leqq P \leqq 1$,

Δ is the thickness, normal to the surface, of the volume of integration,

β is the ratio τ_s/τ_R,

τ_s is the average processing time of the secondary histories,

τ_R is the average processing time of the primary histories,

N_s is the total number of secondary particles produced,

N_p is the total number of primary particles produced.

Even though Dubi attempted to generalize the development several simplifying assumptions were made which resulted in limitations on the use of the benefit factor. The more important assumptions are (1) the correlation between dependent secondary histories, i.e., those produced by the same primary history, is neglected; (2) secondary histories which are produced with an $\bar{n}\cdot\bar{\Omega} < 0$ are neglected, (3) Σ_t^* is assumed to be constant within the volume of integration, and (4) it is required that a history reach the detector location to score, e.g., boundary crossing and analog track length estimators. The analytic benefit factor and its limitations were tested with several sample problem geometries and parameter variations, e.g., thickness of volume of integration, extent of path length biasing, Σ_s/Σ_t ratio, and position of volume of integration. Dubi concluded that there was reasonable agreement between the analytic and experimental benefit factors and that significant advantage may be

gained by use of contributon Monte Carlo estimation. It was cautioned, however, that even though encouraging, the results were not sufficient to "...claim ultimate practical advantages of the contributon method in real-world practical shielding and streaming problems."

Dubi brought out two basic points in his later work which warrant special mention at this point but will be covered in much greater detail in following chapters. First, as a result of the unperturbed transport of the primary particles it is possible to estimate the response simultaneously with the primary histories, i.e., regular Monte Carlo estimation, and secondary histories, i.e., contribution Monte Carlo estimation. At several points in reference 12 the two estimates were referred to as being almost independent, thereby allowing them to be combined to produce a single more precise estimate. However, there was no mathematical basis or significant experimental evidence presented to support this claim. The second point deals with the basis for the apparent advantage in the contributon method. Dubi attributes the advantage completely to the "special new recipe" and not the production of secondary particles. In an attempt to demonstrate this Dubi compared the contributon Monte Carlo method to regular Monte Carlo calculations which included splitting. Regarding these comparisons Dubi states:

> The sole purpose of this was to create as many secondaries as are created by the contributon method in order to demonstrate that the benefit obtained in the contributon scheme is not a result of the generation of secondaries but of the special new recipe used.

The advantage of the contributon method appeared to remain. However, there was no formal basis presented to support Dubi's statement nor was an attempt made to draw any conclusions from the comparisons.

Further application of the contributon procedure was recently reported by Mack and Dudziak[13] who applied the scheme to two practical problems representing simple and complex geometries with moderate to deep penetration. The first is the Fast-Linear Reactor problem which consist of penetration depths of approximately 10 mfp and a complex fusion reactor geometry. Comparisons were made between regular Monte Carlo (RMC) and contributon Monte Carlo (CMC) with exponential biasing and splitting applied to both schemes. Comparisons with parametric variations such as volume of integration thickness in CMC were also made. The authors pointed out that the most important finding was that rule-of-thumb splitting, i.e., factor of two splitting about every mean free path, alone was in general found to be more efficient than CMC. The second problem consisted of a magnetite shield having a relatively simple geometry but penetration depths of 25 to 30 mfp. In this problem the same biasing schemes were applied and varied as in the Fast-Linear Reactor problem. As in the first problem, it was reported that RMC with rule-of-thumb splitting was generally more efficient than CMC. It was further pointed out that CMC with splitting resulted in substantial benefit only when the degree of splitting was much less than rule-of-thumb splitting. Also, the benefit was reported to decrease monotonically as the volume of integration thickness was increased and the degree of splitting approached that of rule-of-thumb.

Deutsch[14] reported comparisons between RMC and CMC performed by a second Los Alamos Scientific Laboratory (LASL) Group, X-6, but performed independently of Dubi and Gerstl. The scope of the X-6 work was primarily limited to the comparison of RMC with geometric splitting and

contributon Monte Carlo. Many of the calculations performed by the LASL Group T-1 (Dubi, et al.) using CMC combined with exponential transform were repeated by the X-6 group replacing exponential transform biasing with geometric splitting. The same calculational indicator of efficiency used by T-1, i.e., the ratio of σ^2T for RMC to σ^2T for CMC, was used for comparison of the X-6 calculations. The results of this work are best summarized by the following quote of Deutsch.

> In essence, the X-6 calculations indicate the absence of any demonstrated value of the T-1 contributon method for the deep-penetration transport problems considered. In these problems, increases in calculational efficiency are not significant and usually a decrease in efficiency is observed. The optimistic conclusion from the earlier T-1 calculations for these problems appear to result from the inefficient treatment of the problems by Monte Carlo without contributions [sic], and specifically from a heavy reliance on the use of the exponential transform as opposed to geometric splitting.

Clearly, the work reported by Deutsch places doubt on the general practical applicability of the contributon Monte Carlo estimator. This doubt serves to point out the need for a thorough understanding of the variance reduction mechanism of the estimator so that its applicability may be assessed. To date, this mechanism has not been given the attention required. Further, the work reported by Deutsch indicates the necessity for development of general guidelines for efficient application of the estimator based on an understanding of the variance reduction mechanism and calculational experience. Development of an understanding of the method for variance reduction by the CMC estimator and guidelines for its effective use are two of the major objectives of the present work.

CHAPTER III

FORMAL BASIS FOR TRACKING AND ESTIMATION PROCEDURES

The purpose of this chapter is to provide insight into contributon Monte Carlo estimation through the formal basis of the tracking procedure. This chapter further demonstrates that the score of Dubi's secondary particles[†] is equivalent to the point value as would normally be calculated in the adjoint mode and, as such, all Monte Carlo procedures, e.g., biasing and estimation, may be applied individually to the SP and ESP random walks.

Dubi[1] has shown that $\eta(p_1,\ldots,p_n)$ as given by equation II-12 (page 11) is an unbiased estimator of the following integral,

$$\int dE \int d\bar{\Omega} \int dV \phi(\bar{r},E,\bar{\Omega})\phi^*(\bar{r},E,\bar{\Omega}) \ . \qquad \text{(III-1)}$$

This is true only when ξ_F^* in equation II-12 is an unbiased estimator of the point value, ϕ^*. The equivalence of ξ_F^* and the point value is based on the relationship between the point and event values, equation II-2 (page 5), the relationship in equation III-2, and an appropriately defined Monte Carlo tracking procedure,

---

[†]As seen in the previous chapter, Dubi refers to the flux estimating particle as the primary particle and the particle produced in the volume of integration as the secondary particle. This author prefers to avoid confusion with the more usual meaning of primary and secondary particle by referring to Dubi's primary particle as the source particle (SP) and Dubi's secondary particle as the equivalent source particle (ESP). The rationale for this terminology will become obvious in the following chapter.

$$\left\langle \xi_c^*(p_1,\ldots,p_k) \right\rangle = \left\langle \sum_{j=1}^{k} g(p_j) \right\rangle = W(p_1), \qquad \text{(III-2)}$$

where:

p_1 is the set of phase space coordinates of the next collision site following emission at p_o, i.e., $p_o = \bar{r}_o, E_o, \bar{\Omega}_o$ and $p_1 = \bar{r}_1, E_o, \bar{\Omega}_o$,

$g(p_j)$ is the ratio $R(p_j)/\Sigma_t(p_j)$,

$R(P_j)$ is the response per unit flux,

$\Sigma_t(p_j)$ is the total cross section at p_j, and

$W(p_1)$ is the event value of a particle with first collision phase space coordinates p_1.

This relationship has been proven by Spanier and Gelbard[15] for a given next collision point. Based on equations II-2 and III-2 ξ_F^* is then defined by the following relationship,

$$\left\langle \xi_F^* (p_o,p_1,\ldots,p_k) \right\rangle = \left\langle T(\bar{r}_o \rightarrow \bar{r}, E_o, \bar{\Omega}_o)\ \delta(\bar{r}-\bar{r}_1)\ \xi_c^*(p,\ldots,p_k) \right\rangle$$

$$= T(\bar{r}_o \rightarrow \bar{r}_1, E_o \bar{\Omega}_o)\ W(\bar{r}_1, E_o, \bar{\Omega}_o) = \phi^*(\bar{r}_o, E_o, \bar{\Omega}_o)\ , \qquad \text{(III-3)}$$

where:

$T(\bar{r}_o \rightarrow \bar{r}, E_o, \bar{\Omega}_o)$ is the transport kernel from point $\bar{r}_o$ to $\bar{r}$ (refer to equation II-2),

$\delta(\bar{r}-\bar{r}_1)$ is the Dirac delta function,

p is a point in phase space, i.e., $\bar{r}, E_o, \bar{\Omega}_o$, and

p_o is the phase space point for ϕ^*, i.e., $\bar{r}_o, E_o, \bar{\Omega}_o$.

The requirements for satisfying equation III-3 then formally define the Monte Carlo tracking procedure for η to be an unbiased estimator of the integral in equation III-1. This relationship is obviously equally valid in the extension of equation III-1 to the calculation of the response as discussed in Chapter II. The estimator used in calculating the response is shown in the following equation,[1]

$$\eta_F(p_1,\ldots,p_n) = \sum_{i=1}^{n} \frac{\chi(\bar{r}_i)}{\Sigma_t(p_i)} (\bar{n}_i\cdot\bar{\Omega}_i) \sum_{j=1}^{k} g(p_j^i)$$

$$= \sum_{i=1}^{n} \frac{\chi(\bar{r}_i)}{\Sigma_t(p_i)} (\bar{n}_i\cdot\bar{\Omega}_i)\, \xi_F^*(p_i,p_1^i,\ldots,p_k^i), \qquad \text{(III-4)}$$

where:

$\chi(\bar{r}_i) = 1$ if $\bar{r}_i$ is within the volume of integration V and 0 otherwise,

$\Sigma_t(p_i)$ is the total cross section,

$\bar{n}_i$ is the outward normal to a surface, containing the collision point and having the same geometry as the bounding surfaces of the volume of integration,

$\bar{\Omega}_i$ is the particle direction vector, and

$g(p_j^i)$ is the response for the j^{th} collision of the ESP produced by the i^{th} collision of the SP.

The tracking procedure for this estimator, as required by the conditions for satisfying equation III-3, is discussed below.

The Monte Carlo scheme used in this work is essentially that outlined in reference 1. This procedure is as follows:

1. The SP is tracked to completion in the normal manner, except that an ESP is produced at each collision site within the volume of integration.
2. At each ESP production site an estimate of the flux, $1/\Sigma_t$, is weighted by $\bar{n}\cdot\bar{\Omega}$, i.e., the flux estimate is transformed to an estimate of the current.
3. The product of the weighted flux estimate from 2. and the SP weight is used as the starting weight of the ESP. The collision phase space coordinates of the SP are taken as the ESP starting phase space values as required by equation III-1.
4. The ESP is tracked in the forward mode to produce an estimate of ξ_F^*.
5. The scores of all ESPs produced by a single SP are summed to produce one independent estimate of η_F.

It is important to note in step 4, that the ESP is tracked in the same manner as the SP. This procedure is implied by equations III-2 and the definition of the event value, i.e., the expected present and future contribution to the effect of interest. It becomes obvious then, as emphasized by the tracking procedure and implied by equation III-3, that the ESP is a direct extension of the SP track prior to the ESP producing collision and is independent of the SP in that they form estimates of different quantities each of which could be determined by separate calculations, as is the normal procedure in the surface integral method discussed in the previous chapter. Therefore, any Monte Carlo biasing or estimation scheme is applicable to the ESP as well as the SP. It must be

cautioned however, that even though the application of biasing is permissible it may not result in a more efficient calculation.

The Radiation Shielding and Information Center's standard version of the MORSE Monte Carlo code[16] was modified to include the ESP production and tracking scheme discussed in this chapter. A variation of this procedure which allows ESP production at a surface crossing has also been included in MORSE. The basis and justification for this variation are developed in Chapter IV. This modified version of MORSE was used exclusively for the Monte Carlo calculations performed in this work.

CHAPTER IV

COMPARISON OF BENEFIT PRODUCING MECHANISMS IN ESP ESTIMATION AND SPLITTING

A prerequisite to the efficient use of any Monte Carlo estimation or biasing scheme is a thorough understanding of the mechanism by which the expected benefit is produced. As stated in Chapter II, Dubi attributes the benefit gained in the contributon Monte Carlo scheme to the "special new recipe" and not intrinsically to the production of the secondary particles, i.e., ESPs. It is the purpose of this chapter to demonstrate that the benefit is derived directly from the production of more than one ESP by each SP, thus showing that the benefit is derived in exactly the same manner in both contributon Monte Carlo estimation and splitting.

Section 1 of this chapter introduces a surface ESP procedure which relies upon a boundary crossing flux estimator rather than the collision density estimator, i.e., volume estimator, used in Dubi's procedure. The benefit producing mechanism of ESP estimation is then demonstrated in Section 2 based on the surface procedure.

1. Surface ESP Estimation

Dubi[1] has shown that the expected value of η_F, equation III-4, is equal to the product of the response and the normal thickness of the volume of integration as shown in equation II-13 (page 12). By replacing the collision density flux estimator in equation III-4 with a boundary crossing flux estimator an equivalent surface ESP procedure may be

defined. Equation IV-1 gives η_S, the surface ESP equivalent of η_F,

$$\eta_S = \sum_{i=1}^{n} \frac{(\bar{n}\cdot\bar{\Omega}_i)}{|\bar{n}\cdot\bar{\Omega}_i|} \sum_{j=1}^{k} g(p_j^i) = \sum_{i=1}^{n} \alpha_i \sum_{j=1}^{k} g(p_j^i)$$

$$= \sum_{i=1}^{n} \alpha_i \xi_F^*(p_i, p_1^i, p_2^i, \ldots, p_k^i) \ , \qquad \text{(IV-1)}$$

where:

$\bar{n}\cdot\bar{\Omega}$ is the angle between the outward normal of the surface and the particle direction vector,

α_i is ± 1, taking the sign of $\bar{n}\cdot\bar{\Omega}_i$, and

all other terms are the same as previously defined.

The tracking scheme for the surface procedure is identical to that of the volume procedure except that ESPs are produced on surface crossings rather than on collisions. This modification does not alter the validity of the equivalence between the expected value of $\xi_F^*(p_o, p_1, \ldots, p_k)$ and the point value $\phi^*(p_o)$ as given by equation III-3 (page 19). The validity is maintained since the equality is independent of the ESP starting phase space coordinates, p_o. As shown in equation IV-2, the expected value of η_S is a direct solution to the response by the surface integral discussed in Chapter II,

$$\langle \eta_S \rangle = \int_{4\pi} d\bar{\Omega} \oint_S dS(\bar{n}\cdot\bar{\Omega})\phi(\bar{r},\bar{\Omega})\phi^*(\bar{r},\bar{\Omega}) = I \qquad \text{(IV-2)}$$

The surface integral in equation IV-2 is the one generally evaluated when the forward and adjoint solutions are determined by

independent calculations, e.g., Williams and Engle.[7] A variation of this surface equivalent source procedure is based on the surface integral used by Hoffman, et al.[10] and a variation of the proof by Case, et al.[9] that the inward directed flux, i.e., that directed toward the detector, uniquely defines the flux field inside the enclosing surface. This procedure differs from the first in that ESPs are only produced on the first crossing of a surface by an SP. The ESPs, however, are tracked in the same manner as in the first surface procedure. Mathematically this is identical to solving the surface integral in equation IV-2 with independent solutions of ϕ and ϕ^*. The forward solution is obtained assuming a vacuum on the detector side of the ESP producing surface and the adjoint solution is obtained without imposing boundary conditions at the ESP producing surface. The integral over $\bar{\Omega}$ is then only performed for angles such that $\bar{n}\cdot\bar{\Omega}>0$. Equation IV-3 gives η_S for this surface procedure,

$$\eta_S = \frac{\beta}{m}\frac{\bar{n}\cdot\bar{\Omega}}{|\bar{n}\cdot\bar{\Omega}|}\sum_{i=1}^{m}\sum_{j=1}^{k} g(p_j^i) = \frac{\beta}{m}\sum_{i=1}^{m}\sum_{j=1}^{k} g(p_j^i)$$

$$= \frac{\beta}{m}\sum_{i=1}^{m} \xi_F^*(p_i, p_1^i, \ldots, p_k^i), \qquad \text{(IV-3)}$$

where:

β is 1 for the first crossing of the surface by an SP and 0 otherwise,

m is the number of ESPs produced per SP crossing, and

all other terms are the same as previously defined.

In equation IV-3 m may be considered to be equivalent to the average value of n in equation IV-1, i.e., the average number of SP collisions in the volume of integration. Equation IV-3 is used in the following section to demonstrate equivalence between the benefit producing mechanisms of splitting and ESP estimation.

2. Method of Benefit Production

To begin, m in equation IV-3 is assumed to be one. For this case equation IV-3 may be written as follows,

$$\eta_S = \xi_F^*(p_1, p_1^1, \ldots, p_k^1). \qquad \text{(IV-4)}$$

In the discussion of the tracking procedure in Chapter III it was noted that ξ_F^* is the continuation of the SP track by the ESP following the collision which produces the ESP or in this case the surface crossing which produces the ESP. In the surface ESP procedure, the initial ESP weight is the SP weight at the surface crossing divided by the number of ESPs produced (assumed here to be one). Taking the Monte Carlo estimate of the expected value of equation IV-4 results in the following relationship which indicates that this procedure is exactly a standard Monte Carlo estimation,

$$[\eta_S] = [\xi_F^*(p_1, p_1^1, \ldots, p_k^1)] = \hat{I} \qquad \text{(IV-5)}$$

where:

[ ] indicates the Monte Carlo estimate of the analytic expected value represented by angle brackets, <>, and

$\hat{I}$ represents the Monte Carlo estimate of the response, I.

Therefore, when each SP produces only one ESP, no benefit is derived from the ESP estimation scheme -- expect possibly that which may be obtained from an additional estimation by the unaltered SP track.

Considering the more general case equation IV-3 may be written as follows,

$$m\,\eta_S = \xi_F^*(p_1, p_1^1, \ldots, p_k^1) + \ldots + \xi_F^*(p_m, p_1^m, \ldots, p_k^m) \ , \qquad \text{(IV-6)}$$

where:

m is the number of ESPs produced by each SP, a fixed integer value greater than one, and

k is variable depending upon the specific ESP track.

Taking the Monte Carlo estimate of the expected value of equation IV-6 results in the following equation,

$$\hat{I} = \frac{1}{m}\left[\xi_F^*(p_1, p_1^1, \ldots, p_k^1)\right] + \ldots + \left[\xi_F^*(p_m, p_1^m, \ldots, p_k^m)\right]$$

$$= \frac{1}{m}\left(\hat{I}_1 + \ldots + \hat{I}_m\right) . \qquad \text{(IV-7)}$$

Equation IV-7 then indicates that each independent estimate ($\hat{I}$) is produced by m dependent estimates ($\hat{I}_1 + \ldots + \hat{I}_m$) each weighted by 1/m, i.e., the arithmetic average of the dependent estimates. The procedure of averaging dependent estimates to produce a single independent estimate is exactly the mechanism used in splitting. In comparison, surface splitting replaces the original souce particle by m dependent particles each with a weight of 1/m times the source particle weight, while the ESP procedure produces m equivalent source particles identical to the split particles and also retains the SP which may be tracked to completion to

yield a separate estimate of the response. The signficance of this difference is discussed in detail in Chapter VII.

It should be noted that with the use of surface crossings as ESP producing events several options are available. The first is as described above, that is, a single surface with multiple ESPs produced per SP crossing. A second is multiple surfaces with one ESP produced per crossing. Obviously, a combination of these options would be equally valid.

The above discussion clearly demonstrates, contrary to Dubi's statement, that the estimation procedure gains its benefit in exactly the same manner and for the same reasons as splitting and not just as a result of the "special new recipe." Further, this discussion clarifies the choice of the terms source particle, SP, and equivalent source particle, ESP, rather than primary and secondary particles. Considering the similarities between this estimation procedure and the standard equivalent source surface integral the procedure will be referred to throughout this work as equivalent source estimation or ESP estimation. It should be obvious that equivalent source estimation unlike most estimation procedures, also includes a biasing scheme. This natural incorporation of biasing into the estimation scheme may then be considered as producing a self-biasing estimator.

The following chapter numerically demonstrates the dependence of benefit on the number of ESPs produced per SP. Also, other similarities are demonstrated between splitting, volumetric ESP estimation (contributon Monte Carlo) and surface ESP estimation.

CHAPTER V

PARAMETRIC STUDIES AND COMPARISONS BETWEEN VOLUME AND SURFACE EQUIVALENT SOURCE ESTIMATION FOR FULL TRANSPORT CALCULATIONS

The calculations leading to the results presented in this chapter had as their bases the four fundamental objectives listed below:

1. Gain insight into the effects on the variance, σ^2, and the $\sigma^2 T$ indicator of efficiency resulting from parametric variations, such as volume position and volume thickness.
2. Demonstrate similarities between equivalent source estimation and splitting.
3. Calculationally demonstrate the dependence of the variance on the number of ESPs produced.
4. Compare surface and volume equivalent source estimation.

The experience gained from the studies reported in this chapter along with that of other investigators, such as reported in Chapter II, will lead to a better understanding of equivalent source estimation and add to the bases for the development of general guidelines for efficient use of the technique.

This chapter is subdivided into five main sections. The first addresses benchmarking of the MORSE Monte Carlo code as modified to perform equivalent source estimation. Sections 2 and 3 report the results of parametric studies for analog (unbiased) and biased calculations, respectively. The final two sections discuss the significance of the results and summarize the main points of the results, comparisons, and discussion.

1. Code Benchmarks

As was mentioned in Chapter IV, the standard RSIC version of the MORSE Monte Carlo code was modified to include options for both volume and surface equivalent source estimation. As good practice dictates, the code was benchmarked following these modifications. For comparison purposes it was necessary in all studies to perform both source particle and equivalent source particle estimates, thus it was only necessary and most efficient to benchmark the source particle estimation with a known solution. Comparison of the SP and ESP estimates of the response for every calculation performed then essentially resulted in a continuing benchmarking of the equivalent source estimators.

Following code modification, standard or SP estimation was benchmarked with the 10 mfp sphere calculation reported by Dubi in reference 11. This problem consist of a homogeneous sphere with a 10 cm radius and an isotropic, monoenergic, point source located at the center. The material within the sphere was assumed to have a total cross section of 1.0 cm^{-1}, an isotropic scattering cross section of 0.9 cm^{-1}, and an absorption cross section of 0.1 cm^{-1}. A vacuum boundary condition was applied at the outer surface of the sphere. Under these conditions Dubi reported a calculated fluence at the outer surface of the sphere of 4.83×10^{-5} particles/cm^2/source particle with a fractional standard deviation (fsd) of 0.015. In the MORSE calculation response estimates were obtained using both last flight and boundary crossing estimators. A 50000 history calculation produced a standard last flight estimate of 4.79×10^{-5} particles/ cm^2/source particle with an fsd of 0.033, while the standard boundary crossing estimator yielded a response estimate of

4.69×10^{-5} particles/cm^2/source particle with an fsd of 0.029. These response estimates consequently verified the validity of both SP last flight and boundary crossing esimation in the modified version of MORSE.

To assure an adequate benchmark of the volume ESP estimator the calculation as described above was repeated using a 5 cm radius sphere with both SP and volume ESP estimation. A 10000 history calculation produced a fluence estimate by SP last flight estimation of 1.45×10^{-3} particles/cm^2/source particle with an fsd of 0.018. The SP boundary crossing estimator produced an identical response estimate and fsd. The volume of integration used for the equivalent source estimation was a spherical shell with inner and outer radii of 0.5 and 1.5 cm, respectively. The ESP last flight estimator yielded a response estimate of 1.50×10^{-3} particles/cm^2/source particle with an fsd of 0.027, while the ESP boundary crossing estimator produced a response estimate of 1.45×10^{-3} particles/cm^2/source particle with an fsd of 0.025. This calculation therefore validated the volume equivalent source option.

2. Parametric Studies for Analog Calculations

This section reports the results of parametric studies specifically for analog, i.e., unbiased, full transport conditions and is aimed at meeting the four objectives outlined at the beginning of this chapter for such conditions. It should be remembered, however, that only the SP estimations are truely analog since the ESP estimations contain the self-biasing mentioned in Chapter IV. These comparisons should most clearly indicate changes resulting from variations in ESP parameters because of the absence of other biasing techniques which might otherwise tend to mask the effects.

The geometric configuration used for all calculations reported in this section was a sphere with a 15 mfp radius and a monoenergetic, isotropic, point source located at the center. The total cross section for the material within the sphere was assumed to be 1.0 cm^{-1} and the isotropic scatter and absorption cross sections were 0.7 cm^{-1} and 0.3 cm^{-1}, respectively. A vacuum boundary condition was applied at the outer surface of the sphere and the normalized fluence was estimated at this surface using both SP and ESP last flight estimation.

Variations in Volume of Integration Position

In this phase of the investigation the position of the volume of integration was varied with respect to the source and detector locations, while the thickness was maintained at a constant 2 mfp. It is important to note that there was no attempt to optimize the volume thickness used in these calculations, in fact, it will be seen in the following subsection that the 2 mfp thickness is a poor choice from an efficiency standpoint. The reason for selecting this thickness was to allow positioning of the volume of integration at as many locations as possible with minimal volume overlap, while still producing sufficient ESPs to obtain reliable results.

To maintain continuity between calculations by providing a consistent base for the $\sigma^2 T$ indicator of efficiency, all calculations were performed using 180000 source particles. As a result of the relatively small number of source particles used in these calculations, estimates of the response were maintained as nearly constant as possible by replacing calculations which yielded unusually high or low estimates of the response, even though statistically the estimates were valid.

This procedure was required since such estimates are generally accompanied by proportionally unusual variances, e.g., high estimates of the response generally result in excessively large variances. It is important to keep the application of this procedure in mind when reviewing the calculated responses so that no additional significance is placed on the tighter than statistically indicated grouping of the estimates. This point is stressed since Dubi in reference 12 noted a similar close grouping in some of his results and stated that "...it may result from the fact that possibly the exact distribution of the scores is not a normal distribution."

The results of the calculations for this phase of the investigation are summarized in Table V-1. The variances and σ^2T indicators of efficiency for the SP and ESP estimators are shown graphically in Figures V-1 and V-2, respectively. The solid curves in these figures represent linear regressions on the Monte Carlo data. The resulting regression equation for the variance is presented in equation V-1, while that for σ^2T is presented in equation V-2,

$$\ln(\sigma^2) = 1.063(-3)x^3 - 1.057(-2)x^2 + 5.322(-2)x - 34.61, \qquad \text{(V-1)}$$

$$\ln(\sigma^2T) = 2.529(-2)x^2 - 0.3489x - 23.80. \qquad \text{(V-2)}$$

The independent variable, x, in both equations represents the number of mean free paths from the center of the sphere to the center of the volume of integration. The significance of the results presented in this subsection will be discussed in Section 4.

Table V-1. Summary of Results for Variations in Position of a 2 mfp Thick Volume of Integration

Position, mfp[A]	Response, particles/cm²/ source particle	Variance	T, sec	Benefit	ESPs Produced
Standard	1.65(-7)[B]	1.61(-15)	11055	--	0
1	1.70(-7)	9.11(-16)	32704	0.60	354506
2	1.69(-7)	1.14(-15)	25395	0.61	276623
4	1.51(-7)	9.50(-16)	17975	1.0	97116
6	1.59(-7)	1.16(-15)	12470	1.2	25896
8	1.51(-7)	1.16(-15)	11075	1.4	6447
10	1.73(-7)	1.76(-15)	10819	0.94	1354
12	1.65(-7)	2.29(-15)	10954	0.71	276
14	1.87(-7)	4.62(-15)	11006	0.35	60
4[C]	1.55(-7)	7.26(-16)	19477	1.3	98424
8[C]	1.67(-7)	9.90(-16)	13493	1.3	6628
10[C]	1.64(-7)	1.07(-15)	12884	1.3	1547

[A]Position corresponds to the center of the volume of integration.

[B]Read as 1.65×10^{-7}.

[C]Surface ESP estimation - Integration over all $\bar{\Omega}$.

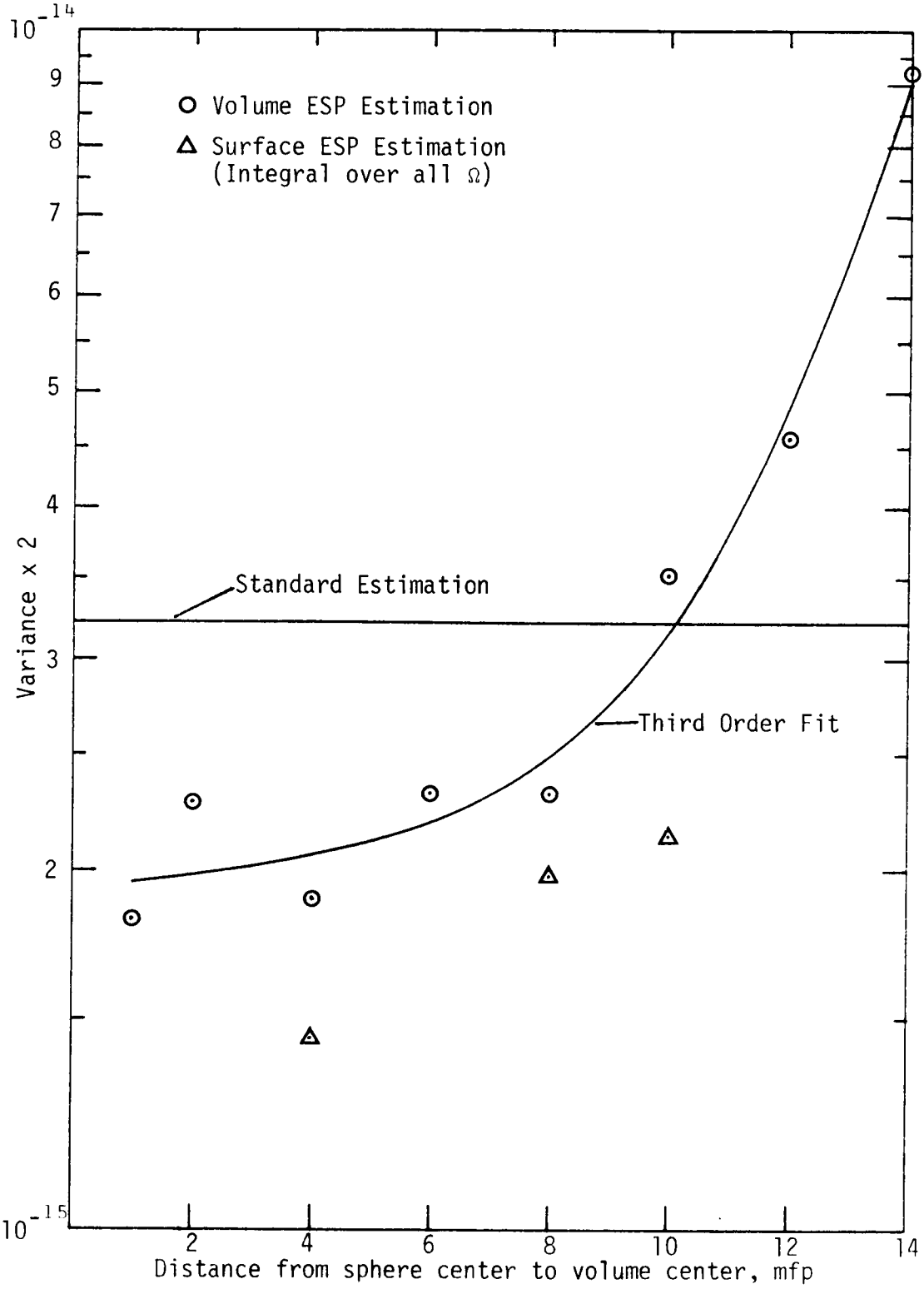


Figure V-1. Variance as a function of ESP volume distance from center of sphere - 2 mfp volume thickness.

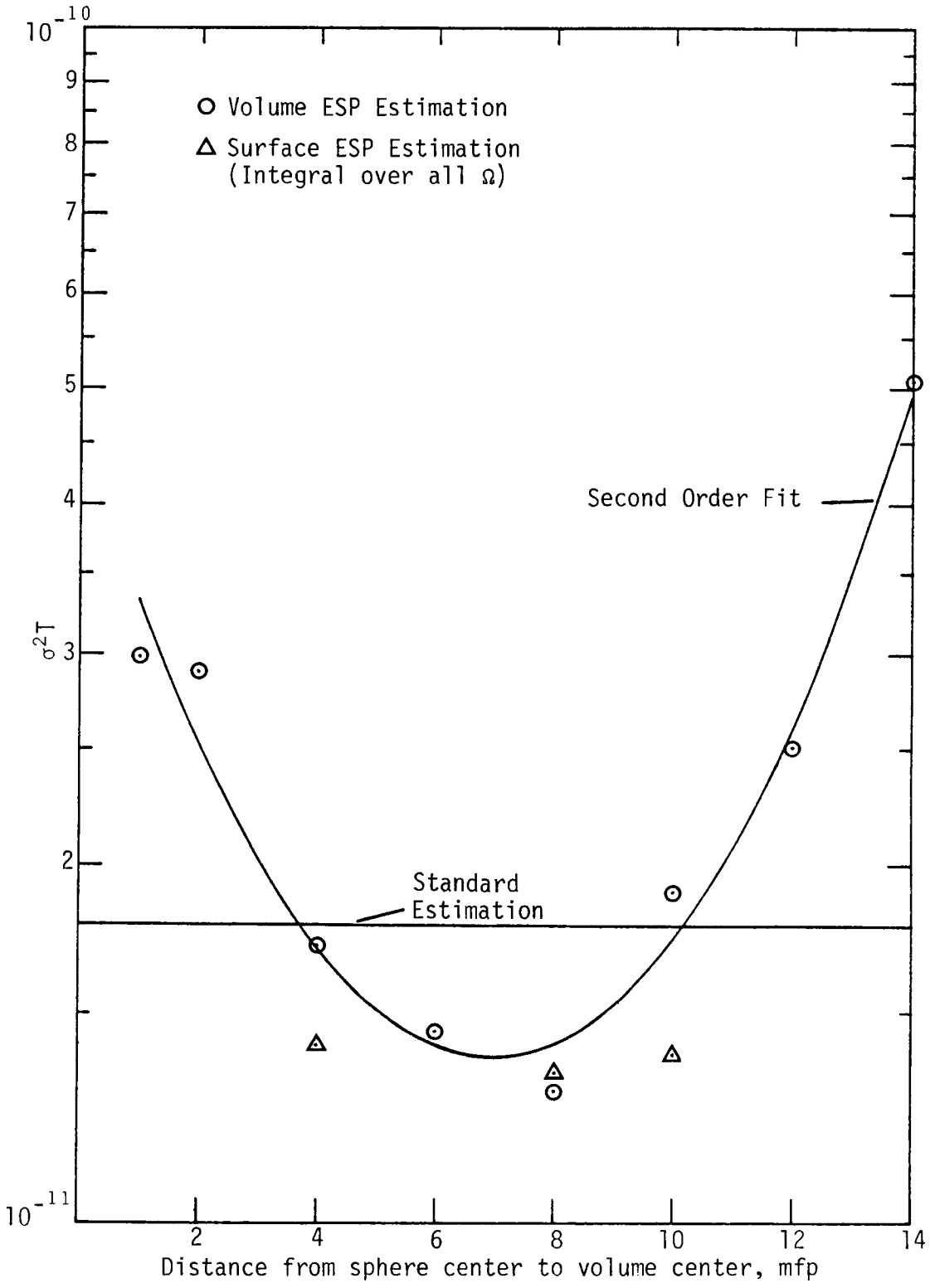


Figure V-2. σ^2T as a function of ESP volume distance from center of sphere - 2 mfp volume thickness.

Variations in Volume of Integration Thickness

In this phase of the study the thickness of the volume of integration was varied about a fixed position. The location of the center of the volume of integration was 7.5 mfp from the source. As seen in Figure V-2 this represents a near optimum position based on the σ^2T indicator of efficiency. For successive calculations the thickness was expanded symmetrically about this location in increments of 1 mfp over a range of 1 to 12 mfp.

As in the previous phase a constant number of source particles, 150000, was used in all calculations. Further, the same procedure was used to eliminate excessive fluctuations in the variance as a result of unusually high or low estimates of the response.

Results of calculations for various volume of integration thicknesses are summarized in Table V-2. The variance and σ^2T indicator of efficiency for these calculations are displayed graphically in Figures V-3 and V-4, respectively, for both the ESP and SP estimators. As before the solid curves in these figures represent linear regressions on the Monte Carlo data. Regression equations for the variance and σ^2T indicator of efficiency are given by equations V-3 and V-4, respectively,

$$\ln(\sigma^2) = 8.213(-3)x^2 - 0.2382x - 33.70, \qquad \text{(V-3)}$$

$$\ln(\sigma^2T) = 1.491(-2)x^2 - 0.2333x - 24.66. \qquad \text{(V-4)}$$

The independent variable, x, in both equations represents the thickness of the volume of integration in mean free paths. The significance of the results for this phase of the study are discussed in Section 4.

Table V-2. Summary of Results for Variations in the Normal Thickness of the Volume of Integration

Thickness, mfp[A]	Response, particles/cm^2/ source particle	Variance	T, sec	Benefit	ESPs Produced
Standard	1.76(-7)[B]	2.14(-15)	9213	--	0
1	1.53(-7)	1.66(-15)	9072	1.3	3733
2	1.61(-7)	1.26(-15)	9713	1.6	7367
3	1.76(-7)	1.22(-15)	9535	1.7	12500
4	1.64(-7)	1.09(-15)	9872	1.8	19269
5	1.74(-7)	8.51(-16)	10489	2.2	27576
6	1.78(-7)	8.07(-16)	10763	2.3	40249
7	1.72(-7)	6.37(-16)	11879	2.6	57384
8	1.82(-7)	5.22(-16)	13213	2.9	79633
9	1.76(-7)	5.15(-16)	15271	2.5	110696
10	1.76(-7)	4.82(-16)	17012	2.4	150845
11	1.68(-7)	4.92(-16)	19522	2.1	201873
12	1.74(-7)	4.34(-16)	23733	1.9	265649
2[C]	1.76(-7)	1.32(-15)	9405	1.6	6779
5[C]	1.72(-7)	5.36(-16)	11340	3.2	25441
8[C]	1.84(-7)	2.26(-16)	14420	6.1	78507
5.5[D] (20)[E]	1.71(-7)	1.81(-16)	12627	5.5	32080
6.25[D] (28)[E]	1.77(-7)	2.43(-16)	13612	6.0	44912
8[D] (49)[E]	1.78(-7)	1.57(-16)	16000	7.8	78841

[A]Thickness expanded symmetrically about a constant center at 7.5 mfp.

[B]Read as 1.76 x 10^{-7}.

[C]Surface ESP estimation - Integration over all $\bar{\Omega}$.

[D]Surface ESP estimation - Integration over $\bar{\Omega}$ such that $\bar{n}\cdot\bar{\Omega}>0$, i.e., vacuum boundary condition at ESP production surface for ϕ calculation.

[E]ESPs generated per SP surface crossing.

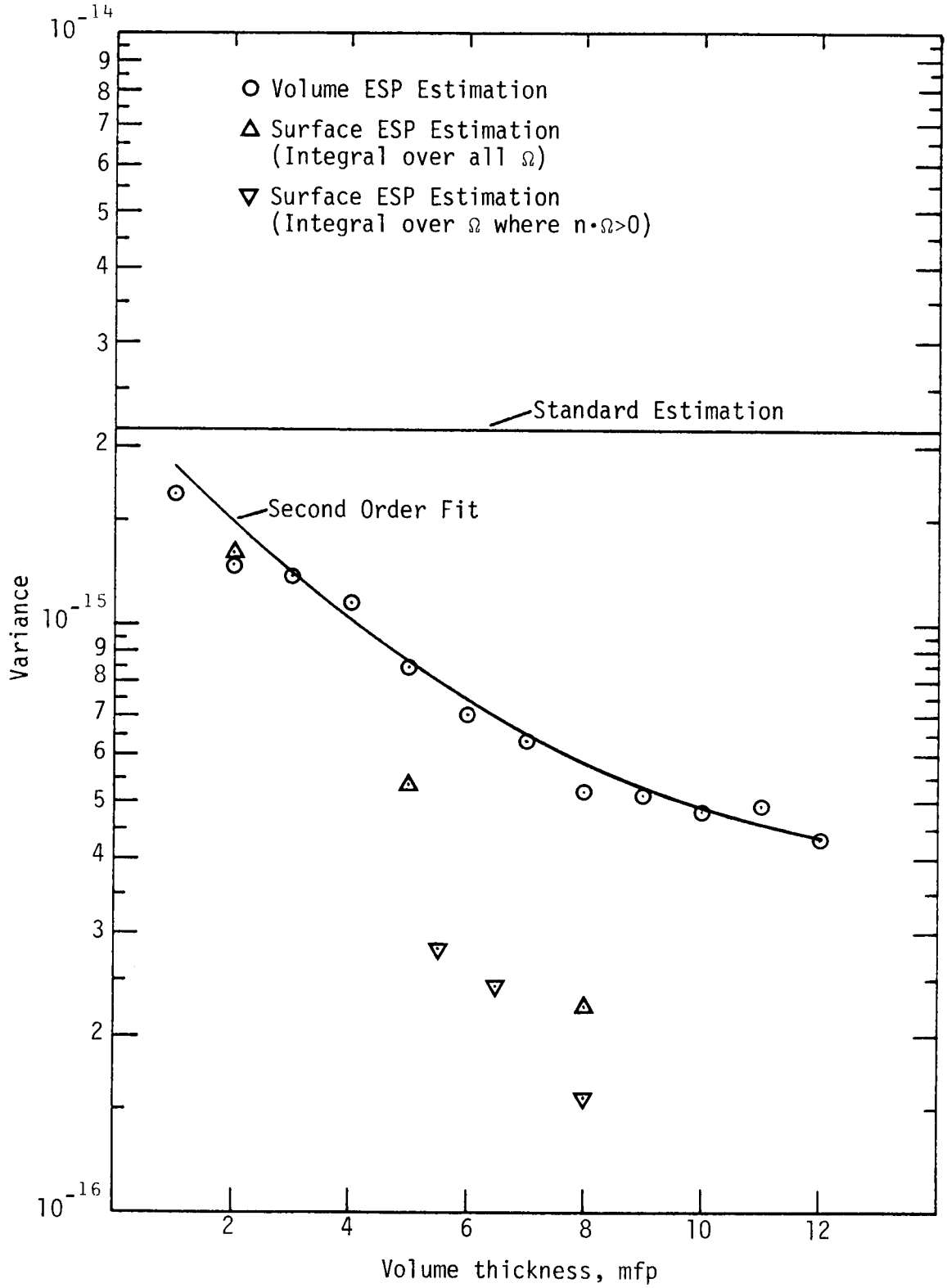


Figure V-3. Variance as a function of ESP volume thickness - volume center 7.5 mfp from sphere center.

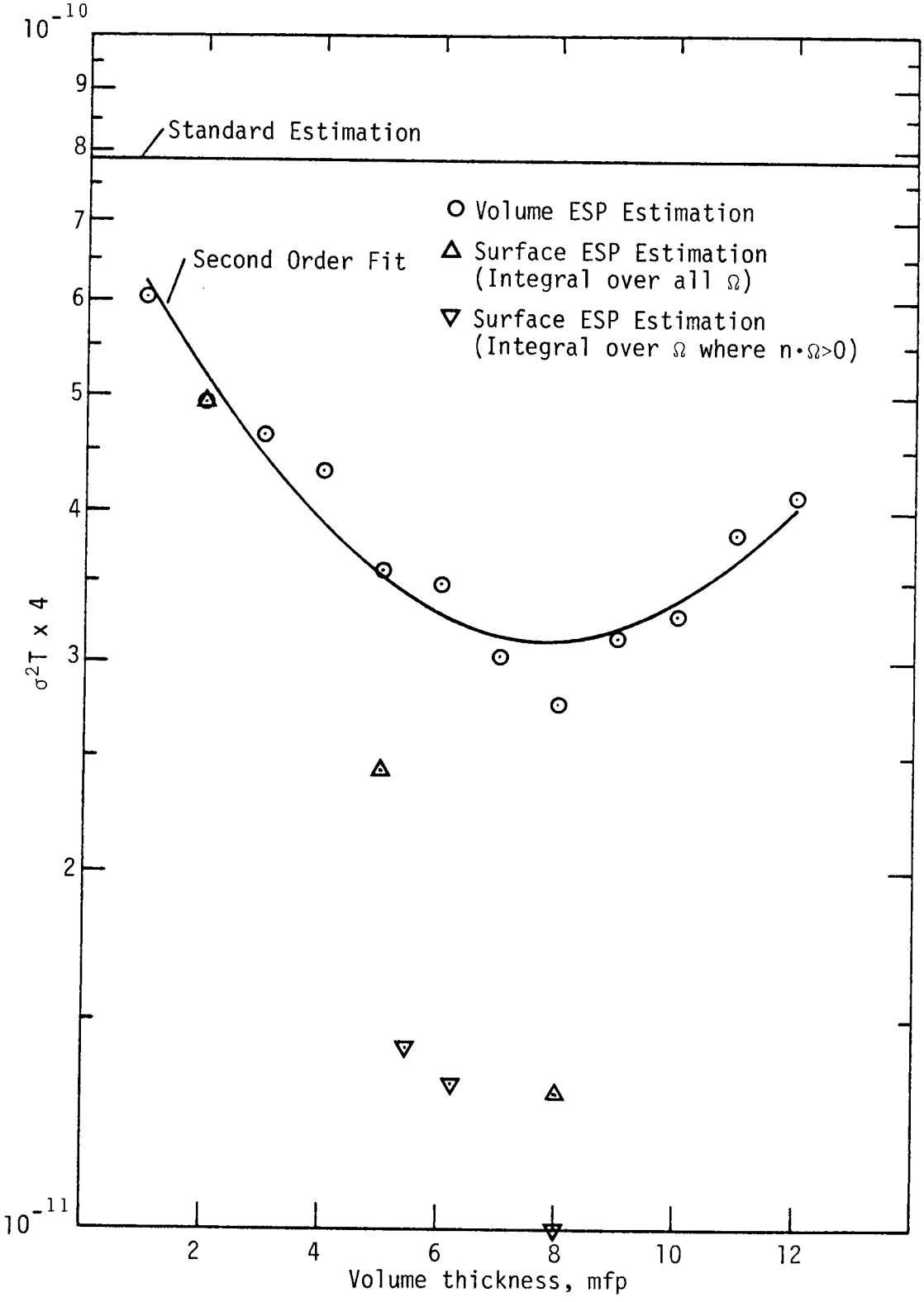


Figure V-4. $\sigma^2 T$ as a function of volume thickness - volume center 7.5 mfp from sphere center.

Comparative Calculations Using Surface ESP Estimation

For comparison purposes calculations using surface equivalent source estimation were performed to correspond with some of the volume ESP calculations discussed in the two previous subsections. Both surface procedures discussed in Chapter IV were employed, i.e., surface ESP estimation requiring integration over all $\bar{\Omega}$ and that requiring integration over $\bar{\Omega}$ such that $\bar{n}\cdot\bar{\Omega}>0$. For convenience the surface procedure requiring integration over all $\bar{\Omega}$ will subsequently be referred to as full surface ESP estimation, while that only requiring angular integration for $\bar{n}\cdot\bar{\Omega}>0$ will be refered to as vacuum surface ESP estimation.

The first set of comparisons were between the volume ESP calculations for variations in volume position and analogous full surface ESP calculations. For the surface procedure the ESP generating surface or equivalent source was located at the same position as the center of the volume of integration for the corresponding volume ESP calculation. Equivalent source locations of 4, 8, and 10 mfp were used. The number of ESPs generated per SP crossing for these calculations was set such that approximately the same total number of ESPs were generated as in the analogous volume ESP calculation. As in the volume procedure, 180000 source particles were used and the same method for reducing fluctuations in the variance as a result of excessive variations in the estimates of the response was employed. The results of the surface ESP calculations are summarized in Table V-1 and the variance and $\sigma^2 T$ values are compared graphically in Figures V-1 and V-2, respectively.

Several surface ESP calculations were performed for comparison with results of volume ESP calculations for variations in volume of integration thickness. In all calculations in this phase 150000 source particles were used and the equivalent source was located 7.5 mfp from the source, corresponding to the location of the center of the volume of integration. As before the number of ESPs generated per SP crossing was set such that approximately the same total number of ESPs was produced as in the corresponding volume ESP calculation. Full surface ESP calculations analogous to volume of integration thicknesses of 2, 5, and 8 mfp were performed.

Calculations employing vacuum equivalent source estimation were also performed for comparison with the volume ESP and full surface ESP calculations discussed in the previous paragraph. These calculations were performed for ESP/SP ratios of 20, 28, and 49, which correspond approximately to 5.5, 6.25, and 8 mfp volume of integration thicknesses, respectively. The value of 28 ESPs generated per SP crossing was determined using a procedure suggested by Carter and Cashwell[17] for estimating the ratio of split particles when employing surface splitting. This procedure is based on the ratio of the importance for the region the particle is entering to that of the region the particle is leaving. The region importance for this determination consisted of the volume averaged adjoint flux which was calculated with the one dimensional discrete ordinates code ANISN.[18] For the geometry used in these calculations, the volume beyond a radius of 7.5 mfp from the source constitutes the region the particle is entering, while the volume inside a radius of 7.5 mfp represents the region the particle is leaving. The ESP/SP ratio of 20

was chosen to represent approximately a 30% reduction in the value estimated by the importance ratio scheme.

The results for the six surface ESP calculations discussed above are summarized in Table V-2 along with the volume ESP results. Grahpical comparisons of the variance and $\sigma^2 T$ are presented in Figures V-3 and V-4, respectively. The significance of all the results present in this subsection will be discussed in Section 4.

3. Parametric Studies for Biased Calculations

This section reports the results of a parametric study performed for biased full transport calculations. The primary objectives of this phase were to (1) gain insight into the use of ESP estimation in biased calculations, (2) determine if the benefit gained in analog calculations remains when biasing is applied, and (3) compare vacuum surface and volume ESP estimation under the condition of biased transport simulation. The biasing applied in these calculations was a combination of nonabsorption weighting, path-length stretching, and Russian roulette. Nonabsorption weighting was the main concern since it is a standard method in the MORSE code and not an input option, i.e., a program modification is required to run MORSE without this form of biasing. Russian roulette was included since nonabsorption weighting forces the tracking of a particle until it escapes unless an alternate mechanism for particle removal is available. Without such a mechanism, the addition of ESP estimation would be expected to result in an increase in computation time which is disproportionate to the decrease in variance.

The geometric configuration, cross sections, and source were the same in this study as for the studies discussed in the previous section. Also, as in the previous studies, the same number of source particles were used in all calculations to maintain continuity by providing a consistent base for the $\sigma^2 T$ indicator of efficiency. For this study 30000 source particles were used in each calculation. Further, the procedure discussed in Section 2 to reduce fluctuations in the variance, which might result because of extreme fluctuations in estimates of the response, was applied as needed. As in all previous calculations last flight estimation was employed for both the SP and ESP procedures.

Path-length stretching was applied uniformly throughout the sphere and equally to the SPs and ESPs in all calculations. It was necessary however, to vary the Russian roulette weight standards between calculations because of variations in the volume of integration position and thickness. For consistency these weight standards were based on the ANISN calculated adjoint flux by use of the following relationships,

$$WA_i = WA_s \frac{\phi_s^*}{\phi_i^*} , \qquad (V\text{-}5)$$

$$WL_i = 0.1\ WA_i , \qquad (V\text{-}6)$$

where:

WA_i is the average weight standard for the i^{th} region,

WA_s is a standard weight at the outer surface of the sphere equal to 7.24×10^{-10} for ESP calculations and 1.08×10^{-8} for the standard calculation,

ϕ_s^* is the adjoint flux at the outer surface of the sphere,

ϕ_i^* is the volume averaged adjoint flux for the i^{th} region, and

WL_i is the low weight standard for the i^{th} region.

All calculations in this study using volume ESP estimation employed the three Russian roulette regions as follows:

1. The equivalent source volume of integration.
2. The volume between the center of the sphere and the inner bounding surface of the volume of integration.
3. The volume between the outer bounding surface of the volume of integration and the outer surface of the sphere.

Calculations using surface ESP estimation employed the same three regions and weight standards as the corresponding volume ESP calculation, i.e., the volume ESP calculation to which the surface calculation was being compared. For the standard calculation the same regions were employed as were used in the optimal volume ESP case.

The first set of calculations performed consisted of variations in the volume of integration thickness. The center of the volume was maintained at a location 12 mfp from the source and the volume thickness was increased symmetrically about the center in increments of 1 mfp to a maximum thickness of 5 mfp. The optimum efficiency, i.e., minimum $\sigma^2 T$, appeared to occur at the 5 mfp volume thickness. Four other equivalent source calculations and a standard calculation were subsequently performed for comparison to the optimum volume ESP case. The first comparitive calculation again utilized a 5 mfp thick volume of integration, but was centered at a location 10.5 mfp from the source. The remaining three calculations all employed vacuum surface equivalent

source estimation. In the first of these the equivalent source was located at the center of the original 5 mfp thick volume of integration, i.e., 12 mfp from the source, and had an ESP/SP ratio of 14, which resulted in a production of approximately the same total number of ESPs as in the volume equivalent source calculation. The flexibility allowed in positioning the surface equivalent source was examined with the final two calculations. In each the equivalent source was located 14.4 mfp from the source, i.e., 0.1 mfp inside the outer edge of the 5 mfp thick volume of integration. The ESP/SP ratios used were 17, resulting in the generation of approximately the same total number of ESPs as in the 5 mfp thick volume case, and 12, representing approximately a 30% reduction in the number of ESPs produced. Table V-3 summarizes the results of all the above calculations, while Figure V-5 graphically compares the variances and σ^2T indicators of efficiency. The solid curves in Figure V-5 represent linear regressions on the Monte Carlo data for the calculations involving variations in the volume of integration thickness. Equations V-7 and V-8 are the resulting regression equations for the variance and σ^2T, respectively,

$$\ln(\sigma^2) = 0.1743x^2 - 1.726x - 33.96, \qquad \text{(V-7)}$$

$$\ln(\sigma^2T) = 0.1607x^2 - 1.501x - 23.91. \qquad \text{(V-8)}$$

The independent variable, x, in both equations represents the volume of integration thickness in mean free paths. The significance of all the results presented in this chapter will be discussed in the following section.

Table V-3. Summary of Results for the Biased Full Transport Calculations

Thickness, mfp[A]	Response, particles/cm^2/ source particle	Variance	T, sec	Benefit	ESPs Produced
Standard	1.52(-7)[B]	6.05(-17)	15657	--	--
1	1.57(-7)	3.48(-16)	28357	9.6(-2)	53959
2	1.61(-7)	1.47(-16)	35002	0.18	111685
3	1.52(-7)	3.62(-17)	39878	0.66	157462
4	1.56(-7)	3.32(-17)	45467	0.63	216475
5	1.49(-7)	2.45(-17)	50870	0.76	257716
5[C]	1.51(-7)	1.95(-17)	64854	0.75	311467
14[D]	1.45(-7)	1.74(-17)	51604	1.1	260232
17[E]	1.49(-7)	2.82(-17)	26753	1.3	251022
12[F]	1.52(-7)	3.53(-17)	25955	1.0	177696

[A] Thickness expanded symmetrically about a constant center of 12 mfp unless otherwise noted.

[B] Read as 1.52 x 10^{-7}.

[C] 5 mfp thickness centered at 10.5 mfp.

[D] Surface at 12 mfp producing 14 ESP/SP.

[E] Surface at 14.4 mfp producing 17 ESP/SP.

[F] Surface at 14.4 mfp producing 12 ESP/SP.

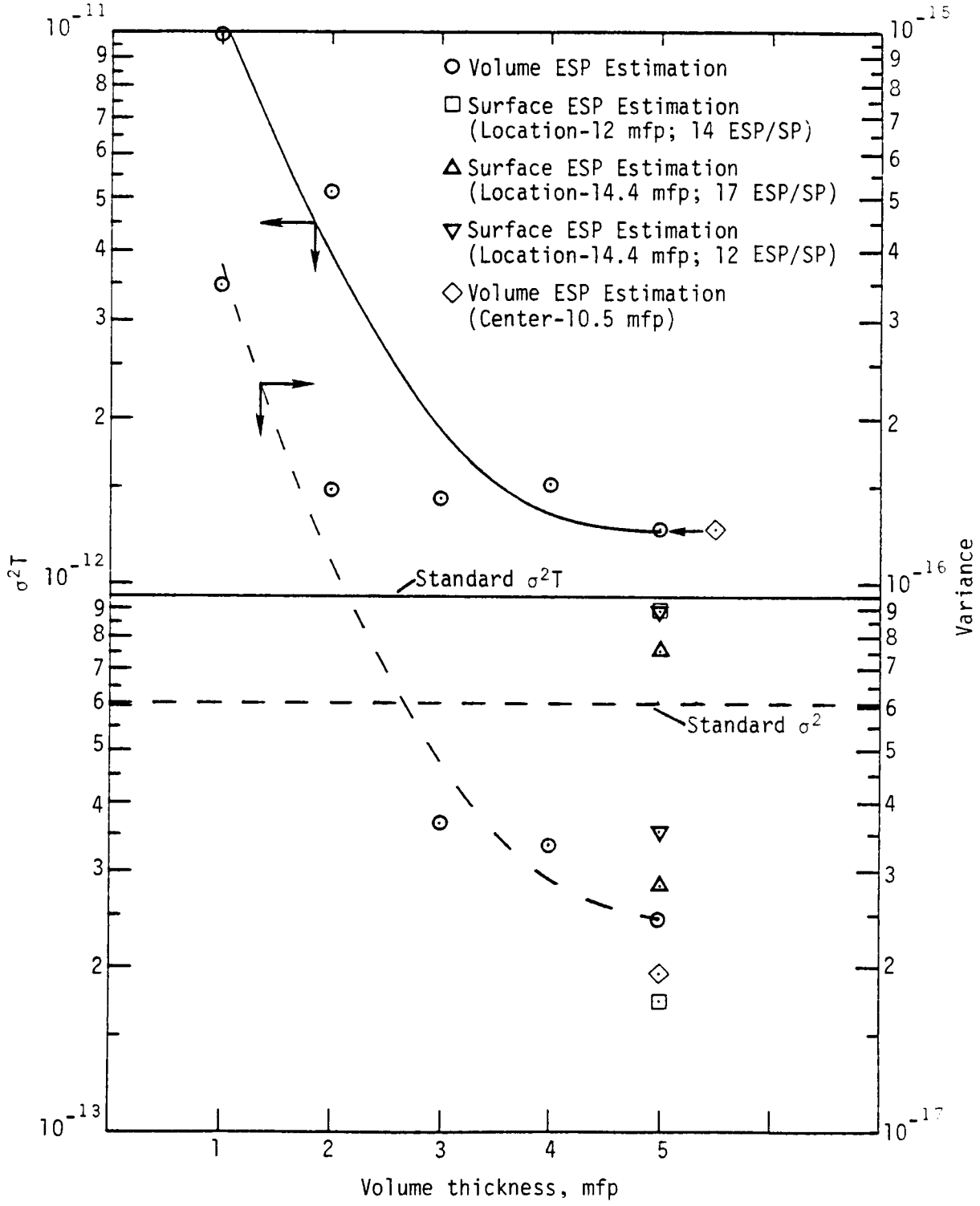


Figure V-5. Variance and $\sigma^2 T$ as functions of volume thickness - biased calculations; volume centered at 12 mfp.

4. Discussion of Results

This section discusses the underlying bases for observed phenomena in the results presented in the previous two sections. A thorough understanding of these bases is required along with an understanding of the variance reduction mechanism developed in Chapter IV in order to establish guidelines for efficient use of the estimators. This discussion will be divided into three subsections. The first two cover the behavior of the variance and $\sigma^2 T$ indicator of efficiency, respectively, for volume ESP estimation. The final subsection deals with comparisons between the volume, full surface, and vacuum surface procedures.

Variance Behavior in Volume ESP Estimation

As noted in the introduction to this chapter, one of the major objectives was the calculational demonstration of the dependence of the variance on the number of ESPs produced. This dependence is clearly shown in Figures V-1 (page 35), V-3 (page 39), and V-5. In each case it should be noted that the variance, at first, rapidly decreases as the number of ESPs produced increases. As should be expected, however, the rate of decline of the variance quickly decreases and the variance asymptotically approaches a minimum value. This value being dependent on the total number of source particles used as well as the use of variance reduction techniques in the calculations.

There are two principle mechanisms responsible for the observed behavior in the variance. The first of these deals directly with the averaging of dependent ESPs, i.e., those within a given ESP group, to

produce a single independent estimate. Increasing the size of the individual ESP groups, that is, increasing the number of ESPs produced, results in each independent estimate becoming more nearly an average estimate, thus resulting in increasingly precise estimates of the response. However, it should be expected, as observed, that beyond a point further increases in ESP group size will result in diminishing returns since most of the independent estimates will begin to approach average estimates. The second mechanism affecting the shape of the variance curve is the predominate cause of the rapid decrease in variance for low ESP/SP ratios. This mechanism consists of increasing the number of independent contributions by increasing the probability of at least one ESP scoring from each ESP group as the group size, i.e., ESP/SP ratio, increases. Obviously this mechanism is only effective up to the point where the ESP/SP ratio has increased sufficiently such that at least one score is obtained from each ESP group. Even though both mechanisms effect the volume and surface ESP estimation procedures, they are not as easily separated in the volume procedure. For this reason, a discussion of the separate mechanisms for a given set of calculations is delayed to Chapter VI. It was necessary, however, to consider these mechanisms at this point in order to understand the observed behavior of the variance.

It is important to note in both Figures V-1 (page 35) and V-5 that in some cases the variance for volume equivalent source estimation may be larger than that produced by standard estimation. This increased variance, which is seen to occur at low ESP/SP ratios, is principally a result of the random method of ESP production in the volume procedure.

This production mechanism results in large numbers of ESPs being produced by particles which undergo many interactions, while very few or even no ESPs may be produced by other particles. In general, those particles which undergo many scatterings are of least interest in deep penetration transport calculations, therefore this procedure biases toward the least interesting histories and, as seen, may produce inefficient results. This inefficiency is discussed again in more detail in the subsection dealing with comparisons between volume and surface ESP estimation.

Behavior of σ^2T in Volume ESP Estimation

This subsection has two primary objectives. The first is to discuss the reasons for the behavior of the σ^2T indicator of efficiency in volume ESP estimation, and the second is to point out a very distinct and important similarity between ESP estimation and splitting.

Figures V-2 (page 36) and V-4 (page 40) indicate what should be expected to be the general shape of the σ^2T curves based on the understanding of the behavior of the variance. In both figures it should be noted that inefficiencies occur in the use of the estimation procedure for both extremes in total ESP production [refer to Table V-1 (page 34) and Table V-2 (page 38)]. For low total ESP production the inefficiency is a result of the relatively large variance, while for the other extreme, i.e., high total ESP production, the inefficiency is a result of rapidly increasing computation time, but only a very slowly decreasing variance. It should be observed that the causes of the inefficiencies are the same for both variations in volume of integration thickness and position. The behavior of σ^2T is seen to be the same for the biased case, Figure V-5, as it is for the analog cases. Although the increase

in σ^2T is not indicated in this figure it should be expected on increasing the volume of integration thickness as supported by the reduced rate of decrease in the variance and the occurrence of equivalent σ^2T values for both 5 mfp thick volume of integration calculations, i.e., volume centers located at 12 and 10.5 mfp.

In late 1979 Juzaitis and Booth[19] reported parametric studies of surface splitting at a single surface in slab geometry. These studies involved variations in slab thickness, number of split particles produced per surface crossing, that is, split particle ratio, and position of the splitting surface. The purpose of the studies was to determine the optimum surface location and split particle ratio based on minimizing the σ^2T indicator of efficiency. Plots of σ^2T as a function of surface position on a normalized scale showed that the optimal position was in the range of 0.5 to 0.7, as was the case in the analog sphere calculations, over the Σ_s to Σ_T ratios considered (0.1 - 0.9). The shape of the σ^2T curves are also seen to be the same as those presented in this chapter, thus indicating the behavioral similarities of σ^2T for surface splitting and volume ESP estimation under variations in surface and volume position. These similarities are highly significant for purposes of developing general guidelines for use of ESP estimation and will be discussed more in Chapter VIII.

Comparisons of Equivalent Source Procedures

It was pointed out earlier that one of the major purposes of the calculations presented in this chapter is a comparison of the volume, full surface, and vacuum surface equivalent source procedures. This subsection performs such a comparison and discusses the underlying reasons for observed differences in the three techniques.

In the graphical presentation of the results of all calculations comparing volume and full surface equivalent source estimation it is readily observable that the full surface procedure results in more precise calculations. One of the causes for the less precise estimates by the volume procedure was mentioned earlier in this section, that is, the random production of ESPs. As discussed, this procedure biases toward the more typical particles and not those of most interest in a deep penetration calculation, i.e., those which undergo very few interactions, and, thus, have the greatest probability of contributing most to the response. In the surface procedure, however, all particles which cross the surface produce the same number of ESPs, thereby, giving all source particles an equal opportunity to contribute to the response. Further, this procedure results in a more uniform number of ESPs being averaged to produce each independent estimate. This, then, eliminates unnecessary over averaging in many ESP groups, while others are under averaged or completely fail to produce a score, i.e., the more uniform ESP group size increases the number of independent estimates that are near average estimates. It should be observed that the reasons just presented for the improved precision of the surface ESP method are very similar to the underlying bases for the shape of the variance curves as discussed in the first subsection of this section. A final cause of the improved precision lies in the knowledge of the equivalent source. In both procedures approximately the same number of independent source particles produce the equivalent source. This results then in a high density surface source and a relatively lower density volume source, therefore, implicitly yielding a more precise integration over the surface equivalent source.

The comparison of vacuum and full surface equivalent source estimation in Figure V-3 (page 39) clearly indicates a more precise calculation by the vacuum surface procedure. Improved precision by this method is not unexpected since part of the surface integral has essentially been performed deterministically. Also in this comparison the total number of ESPs produced by both procedures was approximately constant. For the vacuum surface procedure then the ESP/SP ratio had to be increased since ESPs were only produced on the first crossing of the surface. This enlarged ratio, therefore, increased the probability of obtaining more independent scores as well as allowing more ESPs to be averaged for each independent estimate.

Four final important observations should be made concerning the surface ESP procedures. First, as observed in Figure V-4 (page 40), the optimal ESP/SP ratio has apparently not been reached in the surface procedure when the same total number of ESPs is produced in both the surface and optimal volume calculations. As a result, the increased ratio in the vacuum surface procedure should, as observed, produce a more efficient calculation and not just result in an over production of ESPs. Secondly, it should be noted that in the vacuum surface calculation the ESP/SP ratio is not only increased over that of the analogous full surface calculation, but it is only increased for the more important directions, i.e., those toward the detector. The third observation concerns the use of the region importance ratio to establish the ESP/SP ratio in the vacuum surface procedure. This comparison indicates that the technique does, in fact, result in an adequate estimate of the ESP/SP ratio. Finally, it should be noted in Figure V-5 (page 48) that the

added flexibility in locating the surface equivalent source, over that of positioning the volume of integration, provides an additional increase in efficiency in the surface procedure.

5. Summary

A summary of the most important aspects of this chapter is provided by the following list.

1. The variance has been shown to be dependent on the number of ESPs produced. This noted dependence is a result of three factors, (1) an increasing number of independent estimates as the generation of ESPs increases, (2) improved averaging of dependent estimates as the number of scores from each ESP group increases, and (3) a diminished rate of return for a continued increase in the size of the ESP groups as the larger groups begin to result in estimates which approach average estimates.
2. Volume equivalent source estimation for low total ESP production may provide less precise calculations than standard estimation as a result of the random generation of ESPs.
3. The $\sigma^2 T$ indicator of efficiency was shown to have a distinct minimum which results from the nature of the dependence of the variance on the number of ESPs produced. The shape and minimal value were noted to be very similar to those for surface splitting.

4. It was seen that the benefit gained from volume ESP estimation in the analog case was lost in the biased case considered because of the greatly increased computation time required.
5. Surface ESP estimation was observed to maintain a small benefit in the biased calculation, particularly when advantage was taken of the added flexibility available in locating the surface equivalent source.
6. Volume ESP estimation was noted to be less precise than full surface ESP estimation which in turn was seen to be less precise than the vacuum surface procedure. The principle reasons for the differences were discussed in the third subsection of Section 4.
7. The benefit to be gained by the surface procedures may be greater than indicated since the surface procedures apparently do not reach a minimum in $\sigma^2 T$ for the same total number of ESPs generated as in the optimum volume case.
8. The importance ratio scheme appears to be a viable option for estimating the ESP/SP ratio for vacuum surface equivalent source estimation.

CHAPTER VI

APPLICATION OF VACUUM SURFACE EQUIVALENT SOURCE ESTIMATION TO VOID STREAMING CALCULATIONS

A common application of Monte Carlo transport simulation is in the area of particle streaming in voids. In this class of problem it is often advantageous to eliminate full transport in the material surrounding the void by replacing this material with albedo surfaces, thus, greatly reducing the number of particle interactions and computing time. As a result of the reduced number of interactions by use of albedo surfaces and, in fact, the complete absence of interactions in the most important regions of the geometry, i.e., the void, this class of problem is apparently not amenable to solution by contributon Monte Carlo estimation. It may, however, present an ideal application for the proposed surface equivalent source estimation procedure. This chapter presents the results and discussion of such an application to a two-legged duct geometry. The chapter is organized in two sections. The first is devoted to a description of the problem, and the second presents the results of the calculations and discusses the underlying bases for the observed phenomena.

1. Problem Description

The problem chosen for this investigation consists of a simple but representative void streaming geometry. Figure VI-1 presents a horizontal cross section of the combinatorial geometry model of the two-legged duct used in these calculations. The duct consists of a void

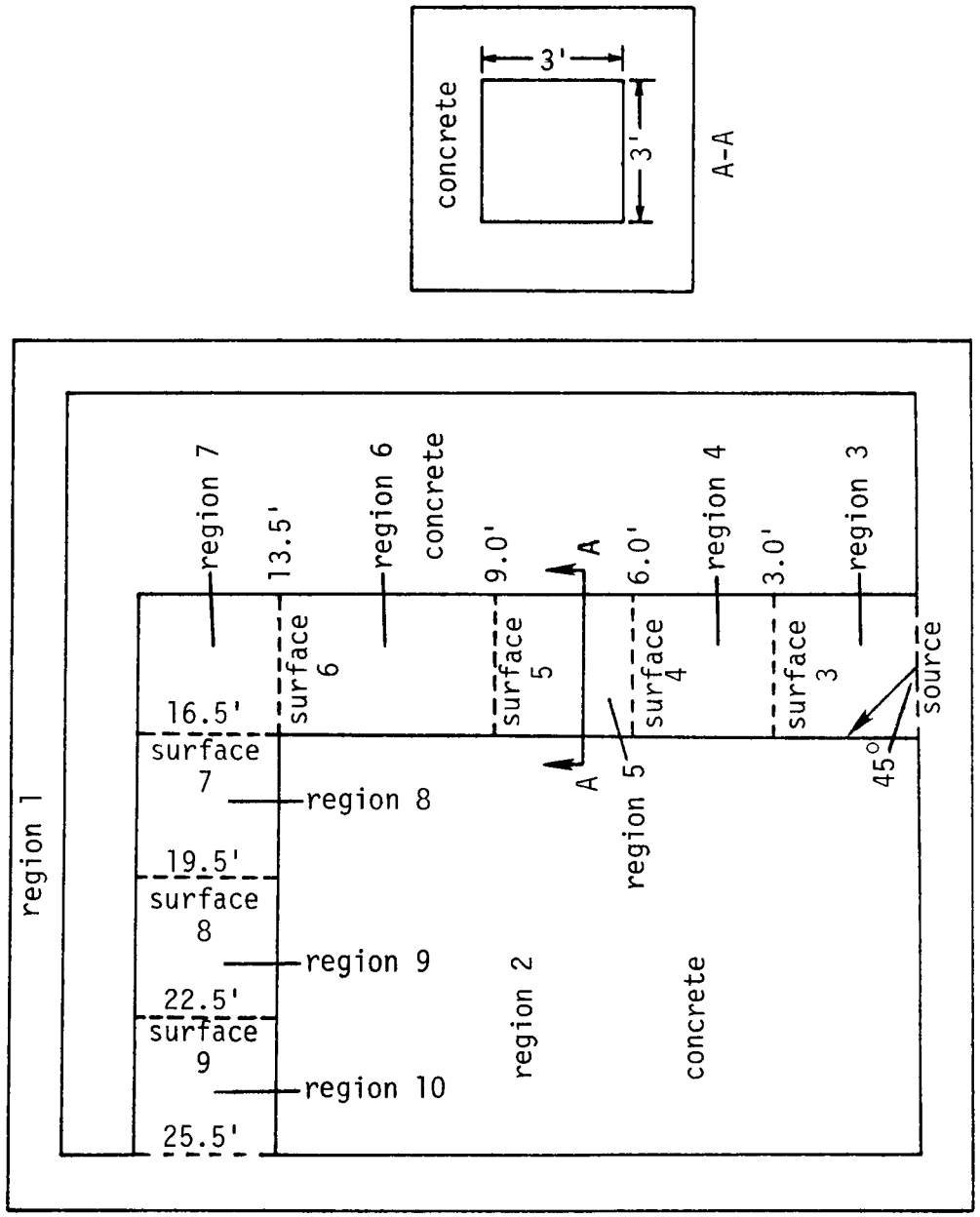


Figure VI-1. Combinatorial geometry model of two-legged duct.

with a 3 ft. by 3 ft. vertical cross section surrounded by concrete walls. The first leg of the duct is 15 feet in length from the entrance to the center line of the second leg, while the second leg is 10.5 feet from the center line of the first leg to the exit.

Full transport in the concrete walls of the duct was eliminated by use of albedo surfaces located at the surface of the duct. To handle the albedo interactions, the BREESE-II[20] routines were incorporated into the modified version of MORSE used for the calculations presented in Chapter V. No modifications to BREESE-II were necessary for use with surface equivalent source estimation since all surface crossings are handled external to the BREESE routines. Therefore, no benchmarking other than comparison of standard and equivalent source estimates of the response was necessary. The one group albedos used by BREESE for all calculations discussed in this chapter were based on the concrete total albedos for the thermal neutron group of the CARP albedo data library.[21] The albedo data set consisted of total albedos for five incident polar angles and differential angular albedos for 30 reflected directions. The angular albedos were developed, for this problem, based on the quadrature weights, as given by equation VI-1,[21] such that isotropic emission from the albedo surface would result,

$$W_{ij} = \frac{\Delta\phi_i \Delta\mu_j}{2\pi} \quad , \qquad \text{(VI-1)}$$

where:

W_{ij} is the weight for the i^{th} polar direction and the j^{th} azimuthal direction,

$\Delta\phi_i$ is the size of the i^{th} reflective polar angle bin, and

$\Delta\mu_j$ is the size of the j^{th} reflective azimuthal cosine bin.

The particle source used in this problem was a monoenergetic, monodirectional, disk source with a radius of 17.32 cm. The source was located in the entrance plane of the first leg and centered on the center line of the leg. As seen in Figure VI-1 the initial particle direction was 45° with respect to the inner wall, thus, adding a degree of difficulty to the problem by increasing the amount of interaction, i.e., attenuation, in the first leg. All calculations reported in this chapter employed 60000 histories. As explained in the last chapter the use of a constant number of histories maintains continuity in the calculations by providing a consistent base for the σ^2T indicator of efficiency.

In this set of calculations the response was the fluence at the exit of the second leg of the duct. The fluence was determined in all calculations using both standard and vacuum surface equivalent source boundary crossing estimation. Since this type of estimator requires the particle to physically cross the boundary to score, it added a further degree of difficulty to the problem, thus, enhancing the need for ESP estimation.

The BREESE routines, like full transport in MORSE, incorporate nonabsorption weighting as a normal mode of operation. For this reason Russian roulette was employed to facilitate particle removal as in the biased calculations discussed in Chapter V. The Russian roulette weight parameters used in these calculations were based on the expected average particle weight for each region shown in Figure VI-1, and were determined for each calculation by the relationships presented in equations VI-2 and VI-3,

$$WA_i = \frac{WR_i}{10N} , \qquad \text{(VI-2)}$$

$$WL_i = 10^{-1} WA_i , \qquad \text{(VI-3)}$$

where:

WA_i is the Russian roulette average weight standard for the i^{th} region,

WR_i is the expected average particle weight for the i^{th} region,

N is the ESP/SP ratio for ESP calculations and one for the standard calculation, and

WL_i is the Russian roulette low weight standard for the i^{th} region.

WR_i was determined for each region from a 22000 history standard calculation designed for this purpose. Since all region volumes remained constant throughout this set of calculations, it was only necessary to modify the weight standards to account for variations in the ESP/SP ratio and not for variations in region volume and position as was the case in the spherical problems when volume ESP estimation was employed. This, then, assures a more uniform application of Russian roulette between calculations. Also, unlike the previous problem, this geometry offered an alternative mechanism for particle removal through leakage out the entrance of the first leg of the duct, thus providing two major sources of particle lose prior to contributing to the response.

Two parametric studies on vacuum surface equivalent source estimation were performed for this problem. The first consisted of

varying the ESP/SP ratio from 3 to 24 for an equivalent source located at the end of the first leg of the duct, i.e., surface 6 in Figure VI-1. The second study involved varying the equivalent source location for a fixed ESP/SP ratio. In this study the equivalent sources were located 9 feet from the source, i.e., surface 5, and 16.5 feet from the source, i.e., surface 7, as well as the previous equivalent source located at surface 6. At each location an ESP/SP ratio of 12 was utilized. For comparison purposes a single standard calculation was also performed. As previously indicated, for the purpose of maintaining continuity each calculation employed 60000 histories and the appropriate Russian roulette weight standards were derived from equations VI-2 and VI-3. The results of all calculations are presented in the following section along with a discussion of important observations and underlying bases for the observed phenomena.

2. Results and Discussion

The results of all calculations performed for the two-legged duct geometry are summarized along with other pertinent associated information in Table VI-1. The variance and computing time for all calculations are displayed graphically in Figure VI-2, while the σ^2T indicators of efficiency are shown in Figure VI-3. As before the solid curves in these figures represent linear regressions on the Monte Carlo data. The resulting regression equations are given by equations VI-4, VI-5, and VI-6 for the variance, computing time, and σ^2T, respectively,

$$\sigma^2 = 2.124(-20)x^2 - 9.583(-19)x + 1.403(-17) \ , \qquad \text{(VI-4)}$$

Table VI-1. Summary of Results for Two-Legged Duct Geometry

ESP/SP[A]	Response, Particles/cm^2/ source particle	Variance	Time, sec	Benefit	ESPs Produced	ESP Groups	Boundary Crossing Estimates
Std	8.30(-8)[B]	2.76(-17)	9187	--	--	--	3264
3	8.59(-8)	1.09(-17)	16440	1.4	33714	11238	7721
6	8.24(-8)	9.55(-18)	23343	1.1	68652	11442	15066
9	8.37(-8)	7.35(-18)	30675	1.1	105651	11739	23176
12	8.72(-8)	5.77(-18)	36325	1.2	141804	11817	30473
15	8.39(-8)	4.04(-18)	42556	1.5	176880	11792	38306
18	8.09(-8)	3.40(-18)	49049	1.5	212994	11833	45292
24	8.51(-8)	3.47(-18)	62404	1.2	290880	12120	61790
12[C]	8.52(-8)	4.31(-18)	50538	1.2	192648	16054	30200
12[D]	8.26(-8)	9.11(-18)	25177	1.1	104916	8743	31974

[A]ESP Surface located 13.5 ft from the source, surface 6, unless otherwise noted.

[B]Read as 8.30(-8)

[C]ESP Surface located at 9.0 ft, surface 5.

[D]ESP Surface located at 16.5 ft, surface 7.

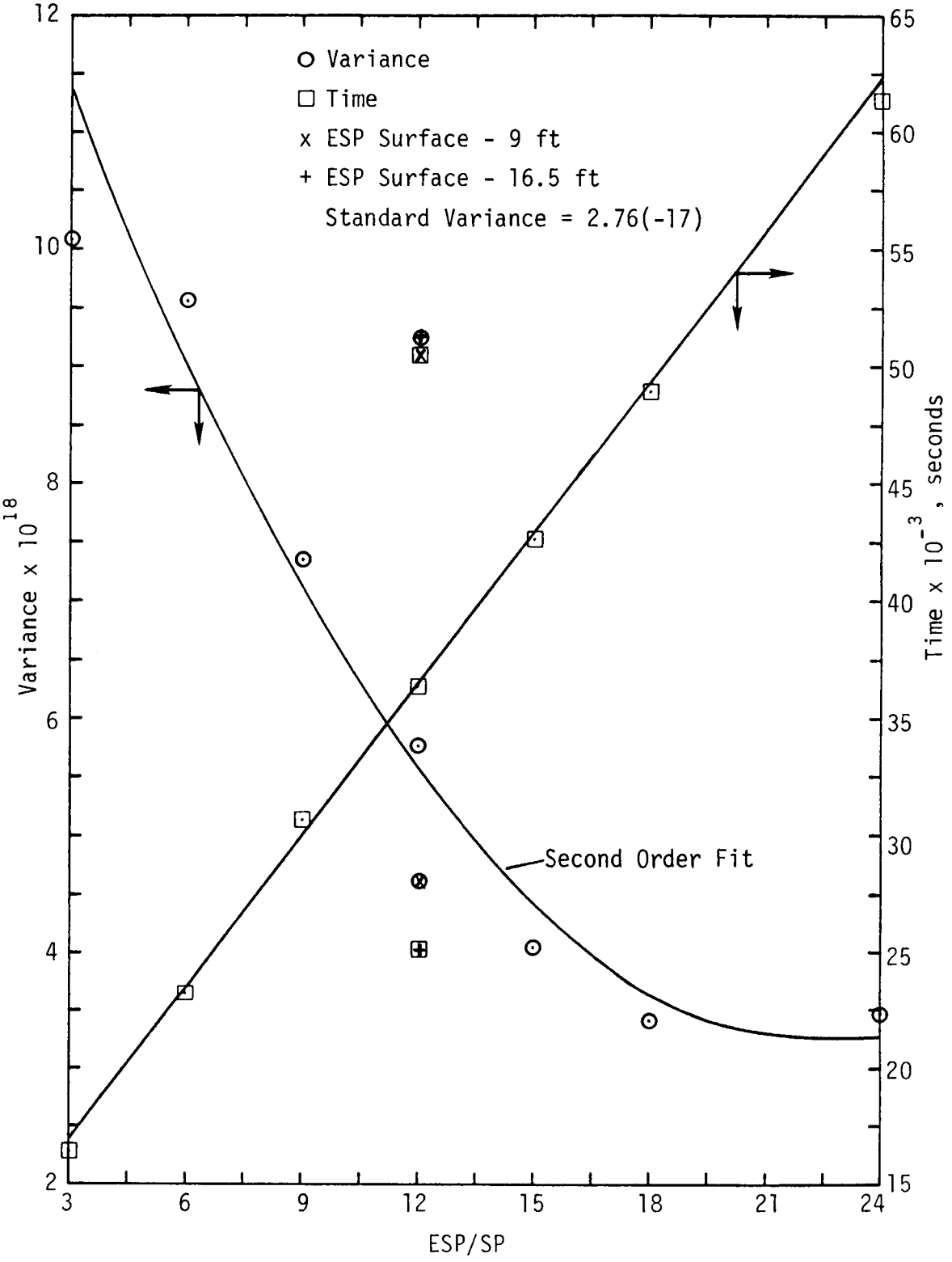


Figure VI-2. Variance and time as functions of ESP/SP ratio - ESP surface located at 13.5 feet.

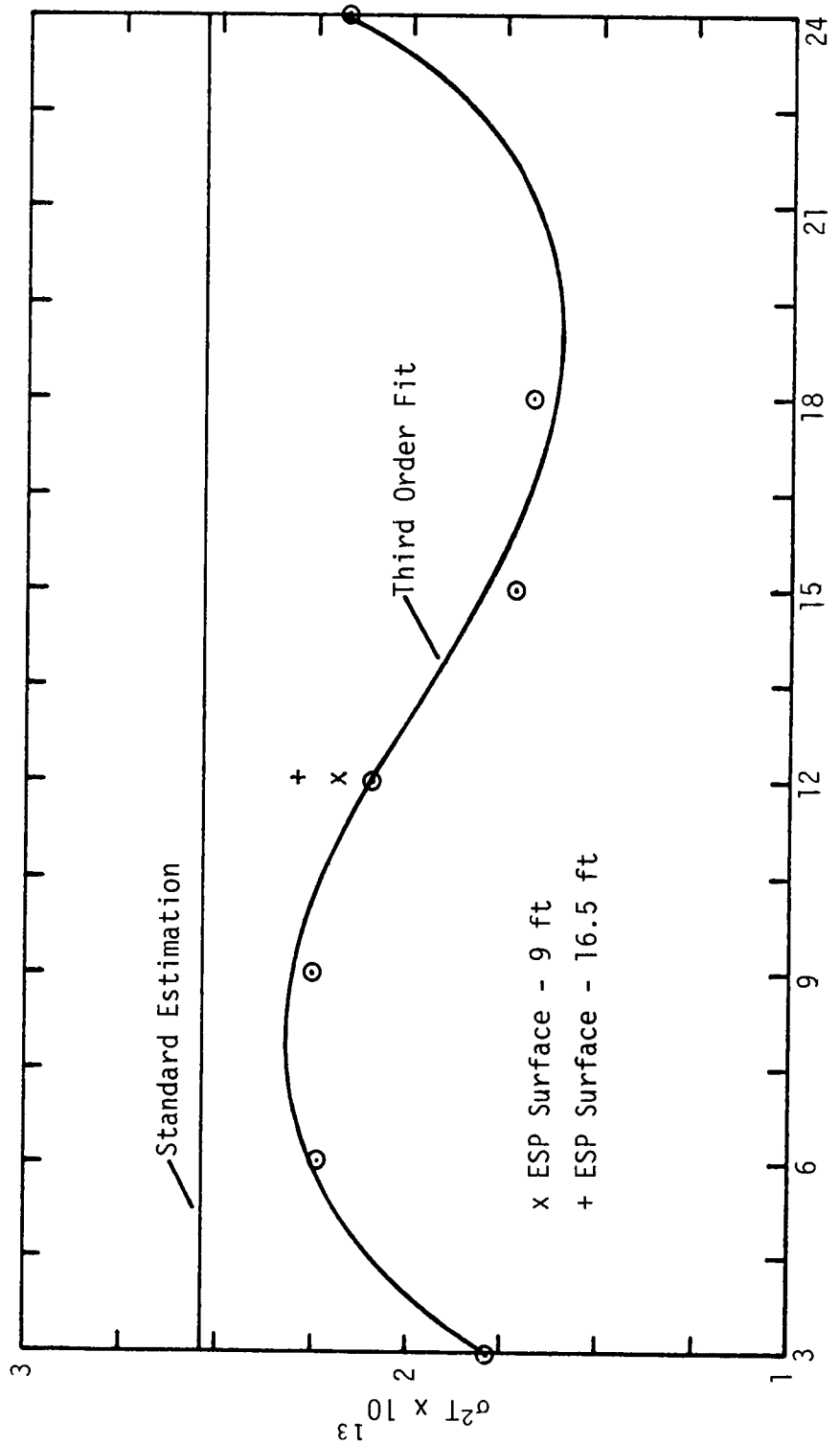


Figure VI-3. $\sigma^2 T$ as a function of ESP/SP ratio - equivalent source located at 13.5 feet.

$$T = 2.164(3)x + 1.036(4) \quad , \qquad \text{(VI-5)}$$

$$\sigma^2 T = 1.060(-16)x^3 - 4.260(-15)x^2 + 4.727(-14)x + 7.243(-14) \quad , \qquad \text{(VI-6)}$$

where:

x is the ESP/SP ratio,

T is the computing time in seconds, and

all other terms are as previously defined.

Figure VI-2 indicates that for an increasing number of ESPs generated, the variance exhibits the same characteristics as were observed in the full transport cases discussed in Chapter V. The underlying causes of this shape, as should be expected, are the same as for the full transport cases. It is also important to note in this figure the significant change in variance resulting from relocation of the equivalent source for the case of an ESP/SP ratio of 12. As determined from Table VI-1 the number of ESP groups represented by the total number of ESPs generated are 16054, 11817, and 8743 for the equivalent source located at surface 5, surface 6, and surface 7, respectively. Also from this table it is seen that each location resulted in approximately the same total number of ESP scores, thus, indicating that more independent estimates were represented for the equivalent source located at surface 5 than at surface 6 and, likewise, more for the equivalent source located at surface 6 than at surface 7. Therefore, clearly and separately demonstrating the variance reduction effect of increasing the number of independent scores as represented in the total number of ESP scores.

The only mechanism for variance reduction for ESP/SP ratios greater than that required to produce, on the average, one ESP score per ESP group is the averaging of dependent estimates. Therefore, this variance reduction mechanism along with the effect of over production of ESPs may be demonstrated separately from the effect of increasing independent scores, as demonstrated in the previous paragraph. The fundamental information for this demonstration is readily obtainable from Table VI-1, that is, the expected number of ESP scores per ESP produced for an equivalent source located at surface 6. This ratio is seen to be approximately 2/9. Therefore, for ESP/SP ratios of 5 or greater it should be expected that the only mechanism affecting the variance is the averaging of dependent estimates. The effects of averaging dependent estimates and the diminishing returns from over production of ESPs is then clearly demonstrated in Figure VI-2 for ESP/SP ratios greater than 5.

It is interesting to note the difference in the shape of the $\sigma^2 T$ curves for the present problem, Figure VI-3, and the full transport cases presented in Chapter V. Primarily the absence of the large inefficiency at low ESP/SP ratios is noted in this problem, thus, resulting in a much flatter curve. This is principally considered to result from the use of the intrinsically more efficient vacuum surface equivalent source estimator and reduced attenuation (from the equivalent source to the detector) in the problem geometry, thereby, allowing more efficient use of each ESP for the computing time. Further, it should be noted that for all ESP/SP ratios, at least to a ratio of 24, the equivalent source

calculation is more efficient than the standard calculation. Based on the shape of the variance and time curves, however, it should be expected that the standard calculation will become more efficient than the equivalent source calculation for ESP/SP ratios greater than 24. A final observation about the $\sigma^2 T$ indicator of efficiency in this problem concerns the calculations for the various equivalent source locations with fixed ESP/SP ratios. It should be noted in Figure VI-3 that the efficiency is approximately the same for all three locations. These observations then indicate the relative insensitivity of the efficiency to both selection of ESP/SP ratio and equivalent source location.

In summary, the behavior of the variance with increasing ESP/SP ratio has been seen to be the same in void streaming and full transport calculations. Further, the fundamental variance reduction mechanisms producing the observed behavior were separately demonstrated calculationally. Regarding the $\sigma^2 T$ indicator of efficiency, it was seen that the curve resulting from increasing ESP/SP ratios did not exhibit the inefficiencies noted for low ESP production in the full transport volume equivalent source cases. Also, a relative insensitivity to ESP/SP ratio and equivalent source location was observed. In conclusion, vacuum equivalent source estimation appears to be a viable option for solution of void streaming calculations.

CHAPTER VII

INVESTIGATION OF THE FEASIBILITY OF COMBINING SIMULTANEOUSLY CALCULATED STANDARD AND EQUIVALENT SOURCE RESPONSE ESTIMATES

As mentioned in Chapter II, Dubi[12] suggested that regular and contributon Monte Carlo estimates may be combined as independent estimates to produce a single more precise estimate of the response. However, he did not provide any mathematical or significant calculational bases for this possibility. In fact, it is not obvious that it would be a reasonable expectation since the equivalent source particles are produced by the source particles, thus, suggesting a possible correlation between the standard and equivalent source estimates. Therefore, this chapter investigates the feasibility of combining results and develops the criteria under which results may be combined to obtain variance reduction by the combination. This investigation is presented in two sections. The first is devoted to development of criteria for the combination of results, and the second calculationally investigates the combination of estimates for the results presented in Chapters V and VI and discusses the general feasibility of combining estimates of the response.

1. Concepts of Combining Correlated Estimates

A fundamental assumption of this investigation is that the equivalent source and standard estimates are dependent and correlated. The methods for combining such estimates are well known and the equations

for combining various moments of the estimates are developed in general terms in such standard texts as Hahn and Shapiro.[22] Because of the nature of the problem being considered, i.e., linear combination of estimates using first order coefficients, the general equations are greatly simplified. Equations VII-1 and VII-2 present the simplified relationships for the first and second moments, i.e., the response and variance of the response, respectively,

$$\phi_c = a_s\phi_s + a_e\phi_e, \qquad \text{(VII-1)}$$

$$\sigma_c^2 = a_s^2\sigma_s^2 + a_e^2\sigma_e^2 + 2\rho a_s a_e \sigma_s \sigma_e, \qquad \text{(VII-2)}$$

where:

ϕ_c is the combined estimate of the response,

ϕ_s and ϕ_e are the source particle and equivalent source particle response estimates, respectively,

a_s and a_e are the SP and ESP coefficients, respectively, with the restriction that $a_e + a_s = 1$,

σ_c^2 is the variance of the combined response estimate,

σ_s^2 and σ_e^2 are the variances of the SP and ESP response estimates, respectively, and

ρ is the correlation coefficient.

The principle objective of combining estimates is to obtain a result which is statistically more precise than either of the individual estimates. Therefore, it is desirable to have a general relationship that indicates if a gain in precision may be obtained. Such an expression is developed by substitution of equation VII-3 into equation VII-2, where equation VII-3 is given by,

$$x = \frac{\sigma_s}{\sigma_e} \quad . \tag{VII-3}$$

For the purpose of this investigation it is assumed that x is greater than or equal to one, i.e., the subscript e is synonymous with the more precise calculation. Equation VII-4 is the resulting expression,

$$g(a_e,\rho,x) = (1 - a_e)^2x^2 + 2a_e(1 - a_e)\rho x + a_e^2, \tag{VII-4}$$

where:

$g(a_e,\rho,x)$ is the ratio σ_c^2/σ_e^2,

$1 - a_e = a_s$, and

all other terms are as previously defined.

As $g(a_e,\rho,x)$ is defined, it is only beneficial to combine estimates of the response when $g(a_e,\rho,x)$ is less than one.

Generally in combining Monte Carlo estimates, the coefficients a_e and a_s are based on the number of histories used for each calculation. The usual relationship for the coefficients is given by,

$$a_i = \frac{N_i}{N_T} \quad , \tag{VII-5}$$

where:

i represents either e or s,

N_i is the number of source particles used in the i^{th} calculation, and

N_T is the total number of histories for the combined calculation, i.e., $N_T = N_s + N_e$.

Using equation VII-5 when combining source and equivalent source estimates results in equal values of a_e and a_s since both estimates are based on the original source, i.e., N_s. Under this condition equation VII-4 may be written as the following equation,

$$g(0.5,\rho,x) = 0.25x^2 + 0.5\rho x + 0.25 \ . \qquad \text{(VII-6)}$$

To investigate the range of values for ρ and x^2, which result in improved precision by combining results, equation VII-6 is displayed graphically as the solid curves in Figure VII-1 for several values of ρ. It should be observed in this figure that the range of x^2 over which an increase in precision may be obtained decreases with increasing correlation and, in fact, for perfect positive correlation no benefit may be gained by combining results. It should further be noted that the constraint to low values of x^2, in order to obtain the greatest benefit from the combination, is contrary to the fundamental objective of biasing, i.e., maximize variance reduction. A final observation is that under the conditions $x^2 = 1.0$ and $\rho = -1.0$, then $g = 0.0$, i.e., the combined variance is 0.0. This observation will be discussed in more detail later.

Figure VII-2 graphically indicates the relationships between ρ and x^2 which allow a more precise estimate by combining results. The solid curve indicates values of ρ and x^2 for which $g(0.5,\rho,x) = 1.0$. Points which fall below this curve will then yield an improved variance upon combining the response estimates.

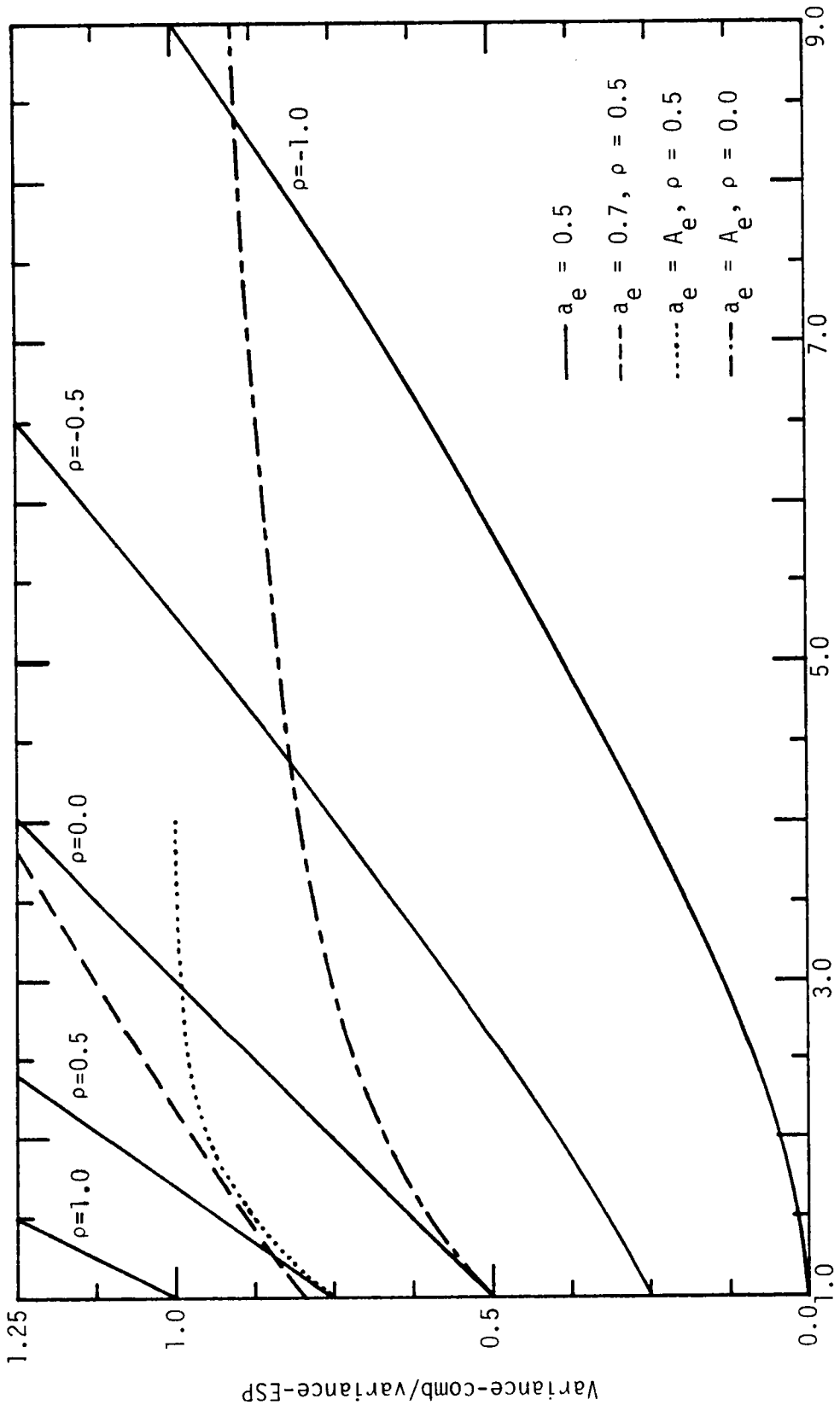


Figure VII-1. Ratio of variance-comb/variance-ESP as a function of the ratio variance-std/variance-ESP and correlation.

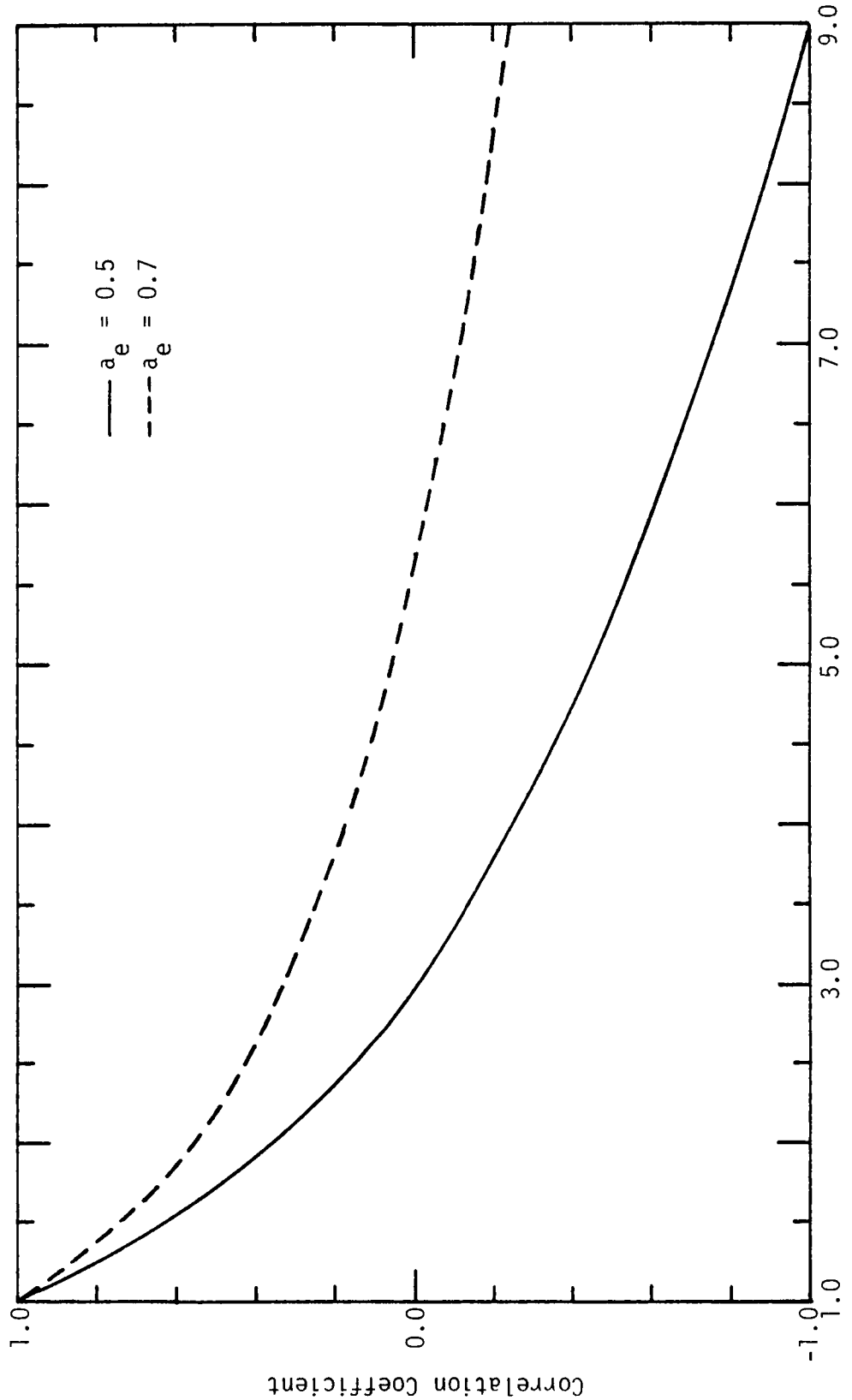


Figure VII-2. Correlation coefficient as a function of the ratio variance-std/variance-ESP for variance-comb/variance-ESP = 1.0.

As mentioned earlier equation VII-5 is the normal relationship used to determine coefficients when combining Monte Carlo response estimates because it weights the combination toward the statistically more precise calculation, i.e., that employing the larger number of histories. However, the coefficients resulting from this procedure are not necessarily the most appropriate for combining SP and ESP estimates since both are weighted equally. An investigation of equation VII-4 for increasing a_e, i.e., increased weighting toward the more precise estimate, indicates an expanded range of ρ and x^2 values for which the combination of estimates is beneficial. The dashed curve in Figure VII-2 is an example of the improved range for the case where $a_e = 0.7$. The corresponding curve for $g(0.7,0.5,x)$ is shown by the dashed line in Figure VII-1. It should be noted in this figure that while the range is expanded, thus providing more benefit for some values of x^2, at the lower values of x^2 the benefit is reduced. This then suggests the existence of an optimum value of a_e, i.e., that which produces the minimum value of $g(a_e,\rho,x)$, for each ρ-x^2 pair.

A general expression has been developed for the optimum value of the coefficient a_e by taking the partial derivative of equation VII-4 with respect to a_e, setting the resulting expression to zero, and solving for a_e. Equation VII-7 is the expression for A_e, i.e., the optimum value of a_e, as a function of ρ and x,

$$A_e = \frac{x(x-\rho)}{x^2-2\rho x+1} \quad . \qquad \text{(VII-7)}$$

As an example of $g(a_e,\rho,x)$ for an optimized combination, equation VII-7 was used with equation VII-4 to produce $g(A_e,0.5,x)$ as indicated in

Figure VII-1 by the dotted curve. It should be noted that even for optimum values of a_e that there is still a limited range of x^2 for which a benefit may be gained when $\rho = 0.5$. This is, in fact, true for all values of ρ greater than zero.

The use of A_e may be generalized by substitution of equation VII-6 into equation VII-4 which then yields the equation,

$$g(A_e,\rho,x) = \frac{x^2(1-\rho^2)}{x^2-2\rho x+1} \quad . \tag{VII-8}$$

Recalling the definition of g, i.e., σ_c^2/σ_e^2, it becomes obvious that equation VII-8 may be used directly to determine the optimum value of σ_c^2. By letting $g(A_e,\rho,x) = 1.0$ a simple inequality may be derived which must be satisfied in order to obtain benefit from combining results and, in fact, must be satisfied in order to assure valid results from equation VII-8. This inequality is given by the equation,

$$\rho \leqq 1/x \quad . \tag{VII-9}$$

As an example of how equation VII-8 may fail if the inequality is not satisfied consider the case where $\rho = 1.0$. For any value of x other than 1.0, equation VII-8 indicates that $\sigma_c^2 = 0.0$. In reality, however, the optimal value of g for $\rho = 1.0$ and any value of x is 1.0.

Two other interesting results are readily obtainable from equation VII-8 for two special values of the correlation coefficient. First, for $\rho = 0.0$ equation VII-8 yields equation VII-10, which indicates that for uncorrelated estimates the use of optimum a_e values produces improved variance for all values of x,

$$g(A_e,0.0,x) = A_e(\rho = 0.0) \ . \qquad \text{(VII-10)}$$

This is, in general, the case for all values of ρ less than or equal to zero. The second observation is for the case of $\rho = -1.0$ and is shown in equation VII-11,

$$g(A_e,-1.0,x) = 0.0 \ . \qquad \text{(VII-11)}$$

Equation VII-11, thus, indicates that the combination of results for any value of x when the estimates are perfectly negatively correlated results in a zero variance estimate. It must be cautioned, however, that the correlation must be a true negative one and not just a value which appears to be statistically indistinguishable from negative one. Thus, like other zero variance estimators, this condition results in an unattainable situation in practice since both the equivalent source and source estimates must have zero or very near zero variances in order to assure a true correlation of negative one. Further, it should be remembered that negative correlation results from a reciprocal relationship between the standard and equivalent source estimates of the response, i.e., lower than average individual standard estimates are, in general, accompanied by individual ESP estimates which are above average and likewise individual SP estimates which are above average are generally accompanied by lower than average ESP estimates. However, since the ESP starting weight is a direct function of the SP weight at the ESP generating event, and since the ESPs and SPs must traverse approximately the same transport medium between the point of ESP production and the detector, it should be expected that the more general

relationship between the standard and equivalent source estimates would be direct. This, thereby, makes any true negative correlations, much less a perfect negative correlation, highly improbable.

2. Application of Concepts and Discussion

For the purpose of calculational investigation into the feasibility of combining equivalent source and standard estimates, the correlation coefficient was included in the equivalent source modifications to the MORSE Monte Carlo code. The correlation coefficient was then obtained as part of each calculation reported in Chapters V and VI. This section is devoted to the application of the concepts developed in the previous section to these calculations, and a general discussion of the feasibility of combining the standard and equivalent source estimates.

Tables VII-1 and VII-2 summarize the results including the correlation coefficient and the $\sigma^2_{max}/\sigma^2_{min}$ ratio, i.e., x^2, for the analog parametric studies of equivalent source position and thickness as discussed in Chapter V. It should be noted in these tables that the correlation coefficients are for the most part nearly zero, and the values of x^2 are such that many estimates could be combined to gain a further reduction in variance. However, it should be further noted that the individual standard variances are generally smaller than the ESP variances, and also that most of the standard response estimates are far below the expected true value. This indicates undersampling in the standard calculations, thus invalidating those estimates and making it incorrect to combine the results with the valid, i.e., more accurate, equivalent source estimates. The occurrence of this situation (i.e.,

Table VII-1. Combination of Results for the Parametric Study on Volume of Integration Position

Position, mfp[A]	Φ_{ESP}	σ^2_{ESP}	Φ_{STD}	σ^2_{STD}	ρ	$\frac{\sigma^2_{max}}{\sigma^2_{min}}$
1	1.70(-7)[B]	9.11(-16)	2.57(-7)	2.44(-14)	-1.3(-2)	27.0
2	1.69(-7)	1.14(-15)	1.19(-7)	1.16(-15)	-6.5(-3)	1.0
4	1.51(-7)	9.50(-16)	1.11(-7)	8.03(-16)	-2.2(-2)	1.2
6	1.59(-7)	1.16(-15)	6.71(-8)	2.55(-16)	-4.0(-3)	4.5
8	1.51(-7)	1.16(-15)	8.10(-8)	4.42(-16)	9.8(-3)	2.6
10	1.73(-7)	1.76(-15)	7.53(-8)	2.82(-16)	-8.7(-4)	6.2
12	1.65(-7)	2.29(-15)	7.52(-8)	2.82(-16)	9.9(-2)	8.1
14	1.87(-7)	4.62(-15)	2.59(-7)	2.42(-14)	0.12	5.2
4[C]	1.55(-7)	7.26(-16)	9.61(-8)	5.03(-16)	2.8(-4)	1.4
8[C]	1.67(-7)	9.90(-16)	1.90(-7)	8.26(-15)	2.3(-3)	8.3
10[C]	1.64(-7)	1.07(-15)	2.06(-7)	8.31(-15)	3.0(-2)	7.7
STD[D]	--	--	1.65(-7)	1.61(-15)	--	--

[A]Location of center of volume of integration unless otherwise indicated.

[B]Read as 1.70×10^{-7}.

[C]Location of surface equivalent source for full surface ESP estimation.

[D]Standard calculation used in Chapter V for unbiased comparisons.

Table VII-2. Combination of Results for the Parametric Study on Volume of Integration Thickness

Thickness, mfp[A]	Φ_{ESP}	σ^2_{ESP}	Φ_{STD}	σ^2_{STD}	ρ	$\frac{\sigma^2_{max}}{\sigma^2_{min}}$
1	1.53(-7)[B]	1.66(-15)	1.24(-7)	1.29(-15)	1.2(-2)	1.3
2	1.61(-7)	1.26(-15)	2.86(-7)	3.47(-14)	-2.3(-3)	28.0
3	1.76(-7)	1.22(-15)	7.65(-8)	5.23(-16)	9.1(-3)	2.3
4	1.64(-7)	1.09(-15)	3.14(-7)	3.50(-14)	-3.7(-3)	32.0
5	1.74(-7)	8.51(-16)	3.21(-7)	3.53(-14)	-4.1(-3)	42.0
6	1.78(-7)	8.07(-16)	2.71(-7)	3.45(-14)	-2.7(-3)	43.0
7	1.72(-7)	6.37(-16)	2.55(-7)	3.44(-14)	-3.5(-3)	54.0
8	1.82(-7)	5.22(-16)	1.26(-7)	1.24(-15)	4.2(-3)	2.4
9	1.76(-7)	5.15(-16)	2.40(-7)	3.42(-14)	-1.7(-3)	66.0
10	1.76(-7)	4.82(-16)	2.54(-7)	3.42(-14)	-8.1(-4)	71.0
11	1.68(-7)	4.92(-16)	1.14(-7)	1.12(-15)	3.2(-2)	2.3
12	1.74(-7)	4.34(-16)	1.14(-7)	1.04(-15)	4.8(-2)	2.4
2[C]	1.76(-7)	1.32(-15)	1.06(-7)	1.02(-15)	4.9(-3)	1.3
5[C]	1.72(-7)	5.36(-16)	1.42(-7)	1.35(-15)	5.3(-2)	2.5
8[C]	1.84(-7)	2.26(-16)	1.21(-7)	9.58(-16)	8.2(-2)	4.2
20[D] (5.5)[E]	1.71(-7)	2.81(-16)	6.93(-8)	6.31(-16)	6.1(-3)	2.2
28[D] (6.25)[E]	1.77(-7)	2.43(-16)	7.49(-8)	2.84(-16)	4.7(-2)	1.2
49[D] (8)[E]	1.78(-7)	1.57(-16)	7.62(-8)	4.65(-16)	5.5(-2)	3.0
STD[F]	--	--	1.76(-7)	2.14(-15)	--	--

[A] Thickness of volume of integration unless otherwise stated.

[B] Read as 1.53×10^{-7}.

[C] Full surface equivalent of volume of integration thickness; surface equivalent source located at center of volume.

[D] Vacuum surface ESP/SP ratio for surface located at 7.5 mfp, i.e., center of volume of integration.

[E] Approximate equivalent volume of integration thickness.

[F] Standard calculation used in Chapter V for unbiased comparisons.

ρ-x^2 pairs that allow combination of results, but involve standard response estimates that indicate undersampling) serves to point out what may well be the general case, particularly when performing analog calculations. This situation should not be unexpected since biasing and techniques such as equivalent source estimation are applied to many problems in order to make the calculations economically feasible. Thus, the number of histories employed is based on obtaining reliable estimates of the response from equivalent source estimation and, therefore, may result in undersampled conditions in the standard estimates.

Undersampling of the standard estimate was not a problem in the biased calculations discussed in Chapter V, but, as was seen, most ESP estimates resulted in less efficient calculations than the standard. Thus, ESP estimation is not a technique that would normally be employed with this type of biasing unless the combined estimates would result in a more efficient calculation than the standard. A summary of pertinent parameters for combining the results of these calculations as well as the combined variances is presented in Table VII-3. The combined variances in this table are given as the inverse of $g(A_e,\rho,x)$, i.e., the amount by which the benefit factors given in Chapter V will be increased. It should be observed in Table VII-3 that only three results satisfy the required inequality for combination of estimates. Even in these cases the combined results were only a minimal improvement, and in no case was the increased precision sufficient to make the equivalent source calculation more efficient than the standard.

The results for combined estimates from the void streaming calculations discussed in Chapter VI are presented in Table VII-4. As was

Table VII-3. Combination of Results for the Parametric Studies with Biased Calculations

Volume Thickness, mfp[A]	Variance-STD	Variance-ESP	Correlation Coefficient	$\frac{\sigma^2_{max}}{\sigma^2_{min}}$	$\frac{1}{g(A_e,\rho,x)}$
1	6.74(-17)[B]	3.48(-16)	0.28	5.2	C
2	6.34(-17)	1.47(-16)	0.72	2.3	C
3	4.03(-17)	3.62(-17)	0.58	1.1	1.16
4	5.41(-17)	3.32(-17)	0.37	1.6	1.08
5	4.51(-17)	2.45(-17)	0.69	1.8	C
5[D]	8.37(-17)	1.95(-17)	0.11	4.3	1.02
14[E]	6.32(-17)	1.74(-17)	0.58	3.6	C
17[F]	5.46(-17)	2.82(-17)	1.3[G]	1.9	C
12[H]	4.77(-17)	3.53(-17)	1.1[G]	1.3	C

[A]Volume centered at 12 mfp.

[B]Read as 6.74×10^{-17}.

[C]Does not meet inequality $\rho \leq \frac{1}{x}$, i.e., equation VII-8.

[D]Volume centered at 10.5 mfp.

[E]Vacuum surface equivalent source located at 12 mfp with ESP/SP ratio of 14.

[F]Vacuum surface equivalent source located at 14.4 mfp with ESP/SP ratio of 17.

[G]Correlation coefficients of greater than 1.0 are a result of statistical fluctuation.

[H]Vacuum surface equivalent source located at 14.4 mfp with ESP/SP ratio of 12.

Table VII-4. Combination of Results for Two-Legged Duct Void Streaming Calculations

ESP/SP[A]	Variance-STD	Variance-ESP	Correlation Coefficient	$\frac{\sigma^2_{STD}}{\sigma^2_{ESP}}$	$\frac{1}{g(A_e,\rho,x)}$
3	2.80(-17)[B]	1.09(-17)	0.24	2.6	1.02
6	2.76(-17)	9.55(-18)	0.43	2.9	C
9	3.49(-17)	7.35(-18)	0.19	4.7	1.00
12	2.44(-17)	5.77(-18)	0.31	4.2	C
15	3.03(-17)	4.04(-18)	0.29	7.5	C
18	3.03(-17)	3.40(-18)	0.25	8.9	C
24	2.58(-17)	3.47(-18)	0.37	7.4	C
12[D]	4.05(-17)	4.31(-18)	0.32	9.4	C
12[E]	3.04(-17)	9.11(-18)	1.6[F]	3.3	C

[A] Equivalent source located at 13.5 feet unless otherwise noted.

[B] Read as 2.80×10^{-17}.

[C] Does not meet inequality $\rho \leqq \frac{1}{\chi}$, i.e., equation VII-8.

[D] Equivalent source located at 9.0 feet.

[E] Equivalent source located at 16.5 feet.

[F] Correlation coefficients of greater than 1.0 are a result of statistical fluctuations.

the case for the biased calculations just discussed, it should be noted that no significant improvement in the variance was obtained in the cases where a combination of the response estimates was allowable. Also, like the biased calculations, all correlation coefficients were positive, thus severely limiting the range and benefit which could be gained by combination of estimates.

In summary, the criteria developed in the first section and the results described above leave little hope for obtaining significant advantage by combining the standard and equivalent source estimates for situations other than those where negative correlation may result. This inability to achieve significant improvement by combination of results for correlations greater than or equal to zero is primarily a result of the fundamental objective of biasing, i.e., maximize x^2 for little or no increase in computing time. It should be expected that this same principle will have a similar minimizing effect on increased benefit in the case of negative correlations. Thus, it is highly likely that the only situations for which combination of estimates will result in significant improvement in benefit are those highly improbable cases for which large negative correlations are obtained.

CHAPTER VIII

GENERAL GUIDELINES FOR USE OF EQUIVALENT SOURCE ESTIMATION

The results presented in Chapters II and V clearly point out the need for general guidelines to assist in avoiding inefficient use of equivalent source estimation. This chapter is devoted to developing such guidelines based on the calculational experience obtained in this research as well as that from previous work, i.e., volume equivalent source estimation, and on the understanding of the variance reduction mechanism developed in Chapter IV and discussed in Chapters V and VI. It must be emphasized that, for the most part, the guidelines presented in this chapter should not be expected to produce optimum efficiency. It is expected, however, that they will provide the user with insight into the behavior of the estimator and will result in parameter estimates which will provide reasonably efficient calculations. Further, it must be recognized that the parameters to be estimated are problem dependent and, therefore, require user knowledge of the particular problem, an understanding of the scheme, and experience or general guidance such as that presented below.

This chapter is organized in three sections. The first summarizes the fundamental principles of equivalent source estimation and their general influence on its use. Specific guidelines based primarily on calculational experience are presented in the second section for the following cases: biasing schemes combined with equivalent source estimation; the selection of an equivalent source location; the selection of an ESP/SP ratio; and combination of standard and equivalent source

estimates of the response. These first two sections present general guidelines and a discussion of the rationale or supporting evidence for the guidelines. The final section presents a brief summary of the most important guidelines for use of equivalent source estimation.

1. Fundamental Principles of Equivalent Source Estimation

In Chapters IV through VI it was concluded that there are basically two fundamental principles which govern the variance reduction in equivalent source estimation. The efficient use of ESP estimation is directly related to a thorough understanding of these principles. In fact, it will be evident that this understanding may well be one of the most efficient tools for deriving equivalent source parameters for practical transport applications.

The first principle was developed in Chapter IV, that is, variance reduction through averaging of constituent dependent estimates to produce independent estimates of the response. Chapters V and VI calculationally demonstrated this principle and further indicated the diminishing return resulting from over averaging. These chapters, as well, demonstrated the second principle, i.e., an increase in the number of independent estimates over the standard calculation by increasing the probability of each source particle contributing, at least partially, to the response. It should be observed that the second principle is dominant in locating the equivalent source, while the first is dominant in determining the ESP/SP ratio. However, both must be considered simultaneously in order to achieve maximum variance reduction without undue increase in computation time.

It is well known that the principles of splitting are essentially the same as those discussed above for equivalent source estimation, therefore, indicating an equivalence between the variance reduction mechanisms of the two techniques. This equivalence is further reinforced by the similarities in behavior of the $\sigma^2 T$ indicator of efficiency. As a result, it was concluded that techniques for determining splitting parameters and calculational experience with splitting may also be applied to equivalent source estimation. This characteristic will be discussed more specifically in the following section.

Two general fundamental points remain to be covered. The first concerns the type of equivalent source estimation to be used. It should be obvious from Chapter V that vacuum surface equivalent source estimation is intrinsically more precise than either the full surface or volume procedures. Further, this procedure is easily employed and is nearly analogous to surface splitting, thus allowing more accurate application of splitting experience and techniques to parameter determination. Therefore, it is recommended that the vacuum surface procedure developed in this research be used in preference to the other techniques. It should be pointed out, however, that an alternate vacuum surface procedure is possible which in some cases may offer advantages over the present procedure. This alternate procedure is briefly discussed in Chapter IX. The last general point concerns the dependence of the benefit on the attenuation. In general, it should be expected that the benefit will increase with increased attenuation. This was observed in calculations performed by Dubi[1] with contributon Monte Carlo for the case of increasing slab and sphere thicknesses, and in those

performed by Juzaitis and Booth[19] with surface splitting for the case of a constant slab thickness and an increasing absorption probability. As an example of the magnitude of this effect, it was observed in calculations by Juzaitis and Booth using a 10 mfp thick slab that a maximum benefit of 3.0 was obtainable when the scattering probability was 0.1, while a maximum benefit of only 1.3 was obtainable when the scattering probability was 0.9.

2. General Guidance of a Problem Specific Nature

This section provides guidance of a problem-dependent nature, for both full transport and void steaming problems. Following the recommendation of the first section, the guidelines presented below are primarily applicable to the vacuum surface equivalent source procedure. The first subsection deals with the use of equivalent source estimation in conjunction with other biasing techniques, and the second and third subsections pertain to locating the equivalent source and the value of the ESP/SP ratio, respectively. The final subsection is directed toward the combination of standard and equivalent source estimates.

Biasing

It should be obvious, based on the equivalence of the variance reduction mechanisms of splitting and equivalent source estimation, that the two techniques would be naturally incompatible when either is near optimum. Therefore, it is recommended that the two procedures not be used in combination. This expected incompatibility is supported by calculational experience as reported by Mack and Dudziak[13] and Deutsch.[14] Mack and Dudziak reported a benefit greater than one for this combination

only when the degree of splitting was far below rule of thumb, i.e., splitting by a factor of two about every mean free path. Deutsch reported similar results, and he further observed that geometric splitting appeared to be more efficient than contributon Monte Carlo. It should be remembered, however, that geometric splitting, i.e., surface splitting, like vacuum surface equivalent source estimation should be considered to be intrinsically more efficient than contributon Monte Carlo. Therefore, the observation made by Deutsch may not reflect the general trend for vacuum surface equivalent source estimation and, in fact, as is briefly discussed in the following chapter, comparisons must be made between geometric splitting and the vacuum surface equivalent source estimators to determine the classes of problems for which each technique is most suitable.

It should be recalled that the variance reduction mechanism of nonabsorption weighting is basically that of increasing the number of independent scores that comprise the estimate of the response. Therefore, resulting in a natural conflict in the schemes by reducing the effectiveness of equivalent source estimation, while greatly increasing the computation time. Calculational experience, however, indicates that there are conditions under which nonabsorption weighting may be used advantageously in combination with equivalent source estimation. The conditions conducive to a combination of the techniques may be inferred from the general behavior of the benefit as presented in the previous section, i.e., increased benefit should be expected with increased particle loss. Therefore, nonabsorption weighting may be employed advantageously if sufficient particle loss occurs, for example: by

leakage prior to contributing; as a result of a high absorption probability resulting in significant loss by Russian roulette over many mean free paths of transport; or by energy cut-off limits. The review of calculational experience, provided in the following paragraph, supports this inference and further supplies insight into the physical parameters which will result in improved benefits when applying survival biasing with equivalent source estimation.

The first problem considered is a parametric study performed by Dubi and Gerstl[12] using contributon Monte Carlo with a cylinderical geometry. The cylinder had a total length of 10 mfp and a point, 2π isotropic source was centered on one end of the cylinder. The volume of integration was a constant 5 mfp thick and, as usual in Dubi's calculations, was attached to the detector which was the cylinder end opposite the source. The transport medium produced isotropic scatter and had a scatter probability of 0.9. Russian roulette was applied in these calculations, thus providing a second means of particle removal. The benefit factor was seen to decrease from approximately 3.7 for a 2 mfp radius to approximately 0.6 for a 12 mfp radius. A benefit factor of one occurred for a radius of approximately 7.5 mfp. Similar calculations were also performed where the volume of integration was allowed to vary along with the radius. In these calculations the same trend was observed, however the benefit was maintained over a wider radius to length ratio. Thus, indicating that possibly a greater benefit and even wider range may be achievable with surface equivalent source estimation because of its greater flexibility with regard to location. Two further examples are the biased sphere and the two-legged duct calculations discussed in Chapters V and VI, respectively. The biased sphere

calculation represents a condition in which Russian roulette was the only particle removal mechanism and a relatively low absorption probability, i.e., 0.3, existed in the transport medium. Under these conditions only marginal benefit was seen to be obtained with vacuum surface equivalent source estimation. The two-legged duct geometry again provided a source of particle removal in addition to the Russian roulette. Unlike the cylinder problems used by Dubi, the particle removal is seen to be more limited, i.e., leakage out the entrance only, yet a significant benefit is still observed to be obtainable. In summary, three criteria are recommended when considering the use of nonabsorption weighting with equivalent source estimation: (1) Russian roulette should always be employed, (2) in cases of low absorption probability additional particle removal mechanisms are required, and (3) in the absence of additional particle removal mechanisms the use should be restricted to high absorption probabilities and large penetration depths, e.g., greater than 15 mfp penetration is required for an absorption probability of 0.3.

Exponential transform, i.e., path-length stretching, is a third commonly employed form of biasing for which some calculational experience has been obtained with contributon Monte Carlo. It was found in both references 12 and 13 that for a constant volume of integration thickness, increasing the transform, i.e., reduced collisions, resulted in a decreasing benefit. This should not be unexpected in contributon Monte Carlo since a reduction in collisions results in a direct reduction in the ESP/SP ratio. This, however, should not be expected to be the case in surface equivalent source estimation since the ESP/SP ratio is not a function of the collision density. In fact, it is expected that

exponential transform will be beneficial when combined with surface equivalent source estimation since one of its main benefit producing mechanisms is a reduction in computation time. Its second mechanism is basically to force particles deeper into the transport medium, thereby potentially allowing placement of the equivalent source closer to the detector. This will result in a further reduction in computation time, while permitting the generation of the same number of independent ESP groups. Even while lacking calculational verification, the combination of these techniques is encouraged based on the understanding and apparent compatability of the benefit production mechanisms.

Most remaining forms of biasing should be compatible with equivalent source estimation, however the use of any biasing technique should be considered on a case by case basis. In general, those techniques which produce benefit by importance sampling, e.g., source energy or position and angular biasing, or by reduction of computation time should be considered to be compatible. However, those techniques which produce benefit by variance reduction, while increasing computation time, may be considered to be incompatible or have only limited compatibility.

Equivalent Source Location

Jazaitis and Booth[19] applied the general theory of Monte Carlo errors to optimizing the location of a surface splitting plane in slab geometry based on minimizing the σ^2T indicator of efficiency. Calculational verification indicated the technique to be accurate within 1 or 2%, i.e., the Monte Carlo values of σ^2 and T were within 1 to 2% of the predicted values. A technique of this nature is also applicable to

the location of a surface equivalent source based on the equivalence of the variance reduction mechanisms of splitting and equivalent source estimation. However, it should be pointed out that this method for locating the equivalent source requires the solution of two integro-differential equations (variance and time) of the same form as the adjoint Boltzmann transport equation. It should be remembered that with a technique such as this, even under the conditions of using fewer spatial dimensions and a less complex geometric model than that used in the actual Monte Carlo analysis, that the cost of determining the optimum equivalent source location may significantly reduce or even nullify any cost savings which might result from the use of ESP estimation. Presently, the only alternative method for location of the equivalent source is an educated guess based on experience, understanding of the variance reduction mechanism, and short trial runs to obtain rough estimates of parameters important in locating the equivalent source. Considering the relative insensitivity of $\sigma^2 T$ to the location of the equivalent source about the optimum, this method should be considered as a very viable and potentially the most cost effective option for locating the equivalent source. For this reason, the remainder of this subsection presents information and a general discussion on important factors for formulating a best guess for the equivalent source location.

In general, selection of the equivalent source location should be considered to be dependent upon the problem and specific biasing techniques which may be employed in its solution. However, for the class of problems with the following characteristics: (1) relatively simple, near homogeneous geometries, (2) near monoenergetic, and (3) strong

particle removal near the source, an equivalent source location midway between the physical source and detector may be appropriate. This location may be inferred from the analog sphere and the two-legged duct problems presented in this work and the slab geometry calculations performed by Juzaitis and Booth.[19] This at first appears to conflict with Dubi's[1,12] recommendation for placing the volume of integration in contributon Monte Carlo as near the detector as possible. However, it should be observed that in most calculations performed by Dubi the volume of integration extends from the detector beyond the geometric midpoint toward the source. Thus, considering the increased flexibility of locating the surface equivalent source, it is suggested that the geometric midpoint may provide an adequate first approximation to the location for most problems. It should be cautioned, however, that problems not providing strong particle removal in the source half of the geometry require that the equivalent source location be shifted toward the detector to prevent excessive computation times. The necessity for this shift is readily observable in the biased sphere problem presented in Chapter V. In cases where equivalent source locations very near the detector are anticipated, e.g., biased sphere problem, the use of ESP estimation is not recommended because of the low probability of obtaining significant gains in benefit.

An important parameter in determining the location of the equivalent source is the fraction of source particles that will produce ESP groups. It has been observed that it is only necessary to produce ESPs with a relatively small fraction of source particles to yield significant reductions in the variance. For example, in the two-legged

duct calculation approximately 19% of the source particles produced ESP groups and with no averaging of dependent estimates, i.e., one ESP score per group, a variance reduction of approximately 2.7 over the standard estimate was obtained. Further, ESP group production by approximately 1.1% of the source particles resulted in a variance reduction factor of approximately 14 in the unbiased sphere calculation for the case of near optimum equivalent source location and ESP/SP ratio. Equivalent source particle production by larger fractions of the source particles results in disproportionate increases in calculational time for the resulting variance recuction.

As discussed in Chapter IV, surface equivalent source estimation allows the option of using multiple equivalent sources. It should be noted that for the case of surface splitting the use of a single optimally positioned surface has been found in many cases to be more advantageous than the use of multiple surfaces with reduced splitting ratios.[19] However, since the optimum location may not be known it may prove to be advantageous to use multiple surfaces. It must be cautioned that the use of multiple surfaces differs in equivalent source estimation and splitting. In the case of splitting the splitting ratio is reduced since the split particles produced at one surface are again split at subsequent surfaces. This, however, is not the case in ESP estimation where only the original source particles produce equivalent source particles at each surface. Therefore, equivalent sources closer to the physical source must employ larger ESP/SP ratios than those closer to the detector to gain advantage. For this reason, a suggested use might be to provide an increase in independent estimates with little or no averaging

by equivalent sources closer to the physical source than the expected optimum location, while sources closer to the detector might be used to provide the averaging effect with the production of fewer ESP groups.

It was mentioned earlier that the selection of the equivalent source location and ESP/SP ratio are not totally separable. It should be recognized that the reliance on calculational experience in the above discussion does, to an extent, intrinsically account for the ESP/SP ratio. After selecting the location and the ESP/SP ratio a short test run should confirm whether compatible parameters have been selected.

ESP/SP Ratio

In general, the determination of the ESP/SP ratio is a more straight forward process than the location of the equivalent source. As seen in Chapter V, the use of the region importance ratio suggested by Carter and Cashwell[17] yields a good, although not optimum, estimate of the ESP/SP ratio when the volume averaged adjoint flux is used as the importance. This method may provide a viable and efficient means of estimating the ESP/SP ratio since in many practical Monte Carlo analyses a single adjoint calculation is performed using a less complex geometric model or fewer spatial dimensions to produce importance information for such schemes as source energy or angular biasing. In many analyses where an adjoint calculation is not practical, an educated guess may be derived from rough parameter estimates determined from a short trial run.

From an understanding of the variance reduction mechanism, it is understood that the minimum desired ESP/SP ratio is that which will result in an average of one score from each ESP group. This minimum

ratio is readily estimated for a fixed equivalent source location by a rough estimate of the attenuation from the equivalent source to the detector. This ratio must then be adjusted by a small integer multiple to allow for averaging of dependent estimates. For example, in the two-legged duct calculation discussed in Chapter VI, the ESP attenuation for an equivalent source located at surface 6 required a minimum ESP/SP ratio of approximately 9/2. Figure VI-3 (page 65) indicates that a reasonable first approximation to the integer multiple might then be in the range of two to five. It should be remembered that the relative insensitivity of $\sigma^2 T$ about the optimum ESP/SP ratio allows error in the estimate of the ratio without significant cost. It is cautioned that this method is most appropriate for use with boundary crossing estimation as used in the two-legged duct calculations. However, it is suggested that the method may be applied to cases using statistical estimation by placing a boundary detector, for use in determining the minimum ratio, a few mean free paths short of the actual detector location, and further, relaxing the integer multiple to assure that over averaging does not occur since the particles are not required to physically reach the detector location.

Combination of Results

This subsection is intended to very briefly outline the important points to be considered in combining the equivalent source and standard estimates of the response. First, the possibility of combining estimates should not, in general, be considered as a means of obtaining a significant increase in benefit. This is a result of the intrinsic incompatibility of the fundamental bases, i.e., maximize x^2 in equivalent

source estimation and maintain x^2 near one to obtain maximum benefit from combining results. Thus, the combination of results should not be a significant factor in the decision to use equivalent source estimation. However, it is recommended that the correlation coefficient be calculated whenever equivalent source estimation is employed since no significant increase in cost is associated with the determination of this parameter. Further, it is recommended that equation VII-8 (page 76) be employed in those cases where combination of results is allowed by equation VII-9 (page 76) such that optimum benefit may be obtained from the combination.

The value of the correlation coefficient is primarily determined by the location of the equivalent source. For this reason, the correlation should be considered when determining the equivalent source location, however it should not be the deciding factor in the choice of location. It should be remembered that increased particle interaction between the equivalent source and detector tends to move the value of the correlation coefficient toward zero.

3. Summary

The most important guidelines for use of equivalent source estimation are summarized briefly in the following list.

1. The form of vacuum surface equivalent source estimation developed in this research is the equivalent source estimator recommended for general use.
2. A combination of splitting and ES estimation is not generally recommended.

3. When nonabsorption weighting is used Russian roulette should always be employed. Further, nonabsorption weighting should only be used when (1) particle removal mechanisms other than Russian roulette are available, e.g., leakage and energy cut-off limits or (2) when low nonabsorption probabilities are combined with deep penetration.
4. For the class of problems which allows significant particle removal near the source an appropriate first approximation to the equivalent source location would be the midpoint between the physical source and detector. With decreased particle removal the equivalent source location should be shifted toward the detector.
5. Equivalent source estimation is not recommended for the class of problems where an equivalent source location very near the detector is anticipated.
6. The region importance ratio method provides a good estimate of the ESP/SP ratio when the volume averaged adjoint flux is used as the region importance. An alternate method is based on adjusting, by a small integer factor, the minimum ESP/SP ratio, as determined by a rough estimate of the ESP attenuation.
7. The combination of standard and equivalent source estimates should not be considered as a means of achieving significant gains in benefit. However, the correlation coefficient should always be calculated and equation VII-8

(page 76) should be employed to determine the combined variance when the criterion of equation VII-9 (page 76) is met.

As a final recommendation, it is best to use conservative parameters for the first calculation in an analysis, i.e., equivalent source located closer to the detector than the anticipated location and a lower ESP/SP ratio than estimated. This procedure will avoid excessive computation time for a given number of source particles and provides insight for adjustment of parameters in subsequent calculations through analysis of the first calculation.

CHAPTER IX

CONCLUSIONS AND RECOMMENDATIONS FOR FUTURE WORK

As a major objective of this research, the full surface and vacuum surface equivalent source estimators were developed as alternatives to contributon Monte Carlo estimation, i.e., volume equivalent source estimation. The variance reduction mechanisms of contributon Monte Carlo and surface equivalent source estimation were investigated. These mechanisms were seen to be equivalent to those of the splitting biasing scheme, that is, an increase in the number of independent scores which comprise the estimate of the response and the averaging of dependent estimates to produce a single independent estimate. The surface equivalent source procedures were seen to be intrinsically more precise than contributon Monte Carlo since (1) all particles crossing the surface produce equivalent source particles, as opposed to the random generation by collision, (2) ESP groups are constant in size, therefore, giving all ESP producing source particles a more equal probability of contributing, and (3) an improved integration over the equivalent source by an increased source density is obtained. It was further seen that the vacuum surface procedure is intrinsically more precise than the full surface procedure as a result of performing part of the equivalent source integral deterministically and increasing the size of the ESP groups for a given total number of ESPs produced.

The feasibility of combining simultaneously calculated standard and equivalent source estimates of the response was investigated as the third objective of this research. It was shown that even for an optimized

combination it is improbable that a significant gain in benefit would be obtained. In fact, it was seen that the fundamentals for obtaining maximum benefit are conflicting, i.e., maximize variance reduction in ESP estimation with minimum increase in computation time, while maintaining the ESP variance to standard variance ratio as near one as possible to obtain maximum benefit from combining estimates of the response.

As the final objective of this work, general guidelines were developed for the use of equivalent source estimation, primarily the vacuum surface form. These guidelines were based on the understanding of the variance reduction mechanisms demonstrated in this research, calculational experience with surface equivalent source estimation, and previously reported experience with contributon Monte Carlo and surface splitting. Although, in general, the guidelines are not expected to produce optimum results they will prevent inefficient use in the following areas: (1) use of vacuum surface equivalent source estimation in combination with other biasing techniques, (2) locating the equivalent source, (3) determining the ESP/SP ratio, and (4) combining the equivalent source and standard estimates of the response.

In conclusion, equivalent source estimation, in particular vacuum surface equivalent source estimation, may be used to gain benefit through variance reduction in many practical fixed source problems involving either full transport or void streaming. However, the areas listed below require further investigation to determine the full potential of the technique.

1. Investigate an alternate form of the vacuum surface equivalent source estimator. This form is equivalent to

calculating the adjoint flux at the equivalent source surface with a nonre-entrant condition on equivalent source particles which cross from the detector side to the source side of the surface, while the inward directed flux, i.e., that direct toward the detector, is calculated without boundary conditions at this surface.

2. Perform comparisons between the vacuum surface equivalent source techniques and surface splitting to determine the most appropriate technique for a given class of problems.
3. Consider the use of separate biasing parameters, e.g., Russian roulette weight standards, for source particles and equivalent source particles.

A potential use of the present form of the vacuum surface equivalent source estimator which is unrelated to the present work is worth mentioning as a final point because of its relatively unique characteristic. As a result of two features of this estimator, (1) potential for high positive correlation between the standard and equivalent source estimates of the response and (2) separate identification of the source and equivalent source particles, this technique may offer a relatively simple, viable option for performing perturbation calculations for many fixed source problems where the perturbation would occur between the equivalent source and detector locations. The positively correlated estimates are desirable to minimize uncertainty between the estimates, other than that resulting from the perturbation, thereby, reducing the masking of small perturbations. Further, the separate identities of the particles allows the use of

different zone properties, e.g., different materials, in the same calculation. It is anticipated that this use may be the only time that it is desirable to use an ESP/SP ratio of one.

LIST OF REFERENCES

LIST OF REFERENCES

1. A. Dubi, S. A. W. Gerstl, and D. J. Dudziak, "Monte Carlo Aspects of Contributons," Nucl. Sci. Eng., 68, 19 (1978).

2. A. F. Henry, Nuclear-Reactor Analysis, The MIT Press, Massachusetts (1975).

3. G. I. Bell and S. Glasstone, Nuclear Reactor Theory, Van Nostrand Reinhold Company, New York (1970).

4. E. A. Straker, P. N. Stevens, D. C. Irving, and V. R. Cain, The MORSE Code - A Multigroup Neutron and Gamma-Ray Monte Carlo Transport Code," ORNL-4585, Oak Ridge National Laboratory (1970).

5. J. S. Tang, T. J. Hoffman, and P. N. Stevens, "Monte Carlo Shielding Calculations Using Event-Value Path-Length Biasing," Nucl. Sci. Eng., 62, 617 (1977).

6. R. R. Coveyou, V. R. Cain, and K. J. Yost, Nucl. Sci. Eng., 27, 219 (1967).

7. M. L. Williams, and W. W. Engle, Jr., "The Concept of Spatial Channel Theory Applied to Reactor Shielding Analysis," ORNL/TM-5467, Oak Ridge National Laboratory (1976).

8. S. A. W. Gerstl, "A New Concept for Deep-Penetration Transport Calculations and Two New Forms of the Neutron Transport Equation," Los Alamos Scientific Laboratory, LA-6628-MS (1976).

9. K. M. Case, F. deHoffmann, and G. Placzek, Introduction to the Theory of Neutron Diffusion, Vol. I, Los Alamos Scientific Laboratory, (1953).

10. T. J. Hoffman, J. C. Robinson, and P. N. Stevens, "The Adjoint Difference Method and Its Application to Deep-Penetration Radiation Transport," Nucl. Sci. Eng., 48, 179 (1972).

11. O. L. Deutsch and L. L. Carter, "Simultaneous Global Calculation of Flux and Importance with Forward Monte Carlo," Fifth Int. Conf. React. Shielding, April 18-23, 1977, Knoxville, Tennessee.

12. A. Dubi and S. A. W. Gerstl, "Application of Biasing Techniques to the Contributon Monte Carlo Method," Nucl. Sci. Eng., 76, 198 (1980).

13. J. M. Mack and D. J. Dudziak, "Applications of Contributon Monte Carlo to Deep-Penetration Transport Problems," Trans. Am. Nucl. Soc., 33, 672 (1979).

14. O. L. Deutsch, "Contributon Monte Carlo at LASL," X-6 Activity Report, July-December, 1979, Los Alamos Scientific Laboratory, LA-8232-PR (1980).

15. J. Spanier and E. M. Gelbard, Monte Carlo Principles and Neutron Transport Problems, Addison-Wesley Publishing, Co., Massachusetts (1969).

16. M. B. Emmett, "The MORSE Monte Carlo Radiation Transport Code System," ORNL-4972, Oak Ridge National Laboratory (1975).

17. L. L. Carter and E. D. Cashwell, Particle-Transport Simulation with the Monte Carlo Method, TID-26607, National Technical Information Service (1975).

18. W. W. Engle, "A Users Manual for ANISN, A One Dimensional Discrete Ordinates Transport Code with Anisotropic Scattering," K-1693, Oak Ridge National Laboratory (1973).

19. R. J. Juzaitis and T. E. Booth, "Minimizing Splitting Costs in Monte Carlo Particle Transport," X-6 Activity Report, July-December, 1979, Los Alamos Scientific Laboratory, LA-8232-PR (1980).

20. V. R. Cain and M. B. Emmett, "BREESE-II: Auxiliary Routines for Implementating the Albedo Option in the MORSE Monte Carlo Code," ORNL/TM-6807, Oak Ridge National Laboratory (1979).

21. M. B. Emmett and W. A. Rhoades, "CARP, A Computer Code and Albedo Data Library for use by BREESE, the MORSE Albedo Package," ORNL/TM-6503, Oak Ridge National Laboratory (1978).

22. G. J. Hahn and S. S. Shapiro, Statistical Models in Engineering, John Wiley and Sons, Inc., New York (1967).

VITA

Robert Sherwood Howell, son of Judge and Mrs. O. D. Howell, Jr., was born February 22, 1949, in Tampa, Florida. Upon completion of H. B. Plant High School, Tampa, Florida he entered the University of Tennessee at Chattanooga where he received his Bachelor of Arts degree in Physics in June 1971. That fall he entered the Graduate School of Texas A&M University and received his Master of Science degree in Nuclear Engineering (Health Physics) in December 1972.

Following completion of his Master's degree he was employed at Kennedy Space Center as the senior health physicist until June 1974 when he accepted a health physics position at Oak Ridge National Laboratory. In September 1976 he left Oak Ridge National Laboratory to continue graduate studies at The University of Tennessee and received the Doctor of Philosophy degree in Nuclear Engineering in June 1981. While in graduate school he joined the Oak Ridge office of Science Applications, Inc.

He is married to the former Donna Jo Avel of Chattanooga, Tennessee. They and their two sons presently reside in Knoxville, Tennessee.